Cargo release from myosin V requires the convergence of parallel pathways that phosphorylate and ubiquitylate the cargo adaptor

Sara Wong[1,2], **Nathaniel L. Hepowit**[3], **Sarah A. Port**[4], **Richard G. Yau**[2], **Yutian Peng**[2], **Nadia Azad**[2], **Alim Habib**[2], **Nofar Harpaz**[5], **Maya Schuldiner**[5], **Frederick M. Hughson**[4], **Jason A. MacGurn**[3], **Lois S. Weisman**[1,2,6,7]

[1.]Cellular and Molecular Biology Graduate Program, University of Michigan, Ann Arbor, MI

[2.]Life Sciences Institute, University of Michigan, Ann Arbor, MI

[3.]Department of Cell and Developmental Biology, Vanderbilt University School of Medicine, Nashville, TN

[4.]Department of Molecular Biology, Princeton University, Princeton, NJ

[5.]Department of Molecular Genetics, Weizmann Institute of Science, Rehovot, Israel

[6.]Cellular and Developmental Biology, University of Michigan, Ann Arbor, MI

Summary

Cellular function requires molecular motors to transport cargoes to their correct intracellular locations. The regulated assembly and disassembly of motor-adaptor complexes ensures that cargoes are loaded at their origin and unloaded at their destination. In *Saccharomyces cerevisiae*, early in the cell cycle, a portion of the vacuole is transported into the emerging bud. This transport requires a myosin V motor, Myo2, which attaches to the vacuole via Vac17, the vacuole specific adaptor protein. Vac17 also binds to Vac8, a vacuolar membrane protein. Once the vacuole is brought to the bud cortex via the Myo2-Vac17-Vac8 complex, Vac17, is degraded and the vacuole is released from Myo2. However, mechanisms governing dissociation of the Myo2-Vac17-Vac8 complex are not well understood. Ubiquitylation of the Vac17 adaptor at the bud cortex provides spatial regulation of vacuole release. Here, we report that ubiquitylation alone is not sufficient for cargo release. We find that a parallel pathway, which initiates on the vacuole, converges with ubiquitylation to release the vacuole from Myo2. Specifically, we show that Yck3 and Vps41,

independent of their known roles in HOPS-mediated vesicle tethering, are required for the phosphorylation of Vac17 in its Myo2 binding domain. These phosphorylation events allow ubiquitylated Vac17 to be released from Myo2 and Vac8. Our data suggest that Vps41 is regulating the phosphorylation of Vac17 via Yck3, a casein kinase I, and likely another unknown kinase. That parallel pathways are required to release the vacuole from Myo2 suggests that multiple signals are integrated to terminate organelle inheritance.

Graphical Abstract

Cla4 and Dma1 regulate ubiquitylation of Vac17

Yck3 and Vps41 regulate phosphorylation of Vac17

Vac17 is released from the complex and degraded by the proteasome
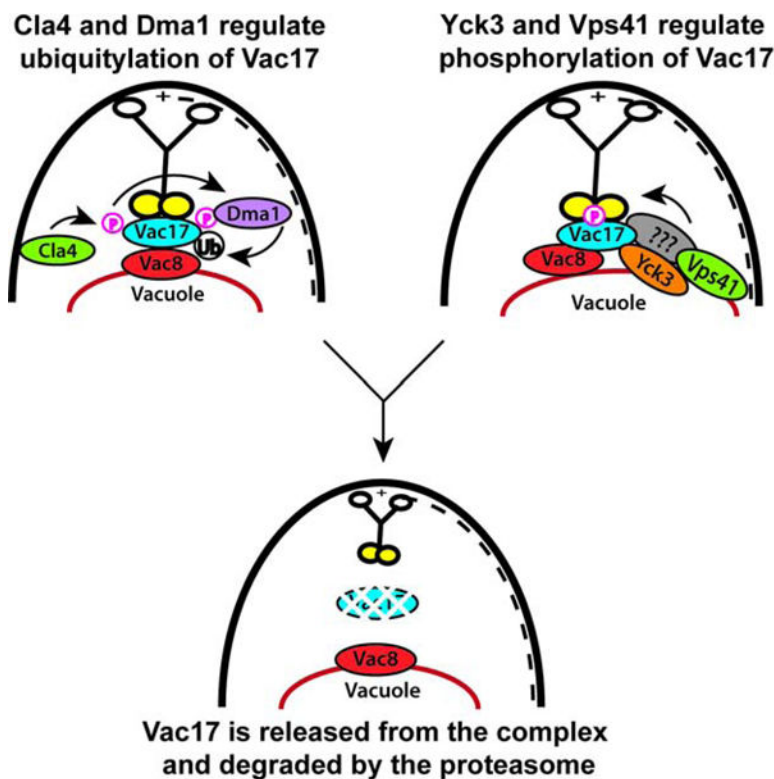
eTOC Blurb

After delivery, cargo is uncoupled from its molecular motor via a pathway that requires ubiquitylation of the adaptor protein. Here, Wong et al. discover that this is not sufficient, and a second, parallel pathway also acts on the adaptor. They show that convergence of both pathways is required to release the vacuole cargo from the myosin V motor.

Keywords

Myosin V; Myo2; Cargo Adaptor; Organelle Transport; Vacuole Inheritance; Protein Degradation; Vac17; Vac8

Introduction

Myosin V motors transport organelles to their correct intracellular locations. In *Saccharomyces cerevisiae*, a myosin V, Myo2, transports the vacuole [1, 2], mitochondria

[3], peroxisomes [4], secretory vesicles [5], Golgi [6], astral microtubules [7–11], and lipid droplets [12] to the bud during cell division. Transport initiates when myosin V binds to cargo-specific adaptors and attaches to organelles [13–15]. Upon reaching their destinations, organelles are detached from myosin V, thereby terminating transport.

Vacuole transport in yeast is a highly regulated process. The vacuole-specific cargo adaptor, Vac17, physically links Myo2 to the vacuole [16, 17]. Early in the cell cycle, Vac17 is phosphorylated by Cdk1, which facilitates Vac17 association with Myo2 [18]. Vac17 binds to the vacuole via Vac8, a vacuolar membrane protein [19–21]. Formation of the Myo2-Vac17-Vac8 complex bridges the vacuole to Myo2 and allows a portion of the vacuole to be brought into the growing bud. Later in the cell cycle, Myo2 is released from the vacuole via the regulation of Vac17. At the bud cortex, a bud-cortex localized kinase, Cla4, phosphorylates Vac17 [22]. This spatial cue signals the proper delivery of the vacuole to the bud. Vac17 is then ubiquitylated by the E3 ligase Dma1, which targets Vac17 for degradation by the proteasome [22]. In mutants where Vac17 is not degraded, Myo2 is not released from the vacuole [17, 22]. It was previously assumed that ubiquitylation is both necessary and sufficient for the termination of vacuole transport.

Here, we report a pathway that functions in parallel with the ubiquitylation of Vac17 to dissociate Vac17 from the Myo2-Vac17-Vac8 complex. We show that the homotypic fusion and protein-sorting (HOPS) subunit, Vps41, regulates an unknown kinase and the vacuole-localized Casein Kinase I, Yck3, to phosphorylate Vac17. These phosphorylation sites on Vac17 are required for the release of Vac17 and its delivery to the proteasome for its subsequent degradation. However, Myo2 and Vac8 are not degraded and remain in their original locations. This suggests that Vps41 and Yck3 regulate the dissociation of ubiquitylated Vac17 from the motor-adaptor complex. We find that ubiquitylation of Vac17 occurs independently of Vps41 or Yck3. Conversely, Vps41 and Yck3 -dependent phosphorylation occurs without ubiquitylation. However, both the Vps41 and Yck3 -dependent pathways and the ubiquitylation pathway are required for the vacuole to be released from Myo2 and for Vac17 to be degraded. We predict that the dissociation of myosin V from other cargo adaptors, in yeast and mammals, undergo similar types of regulation. These studies reveal that the termination of cargo transport is tightly controlled. Moreover, these studies predict that release of cargoes from molecular motors is critical to cellular health and function.

Results

Yck3 and Vps41 regulate the termination of vacuole transport

Vac17 is highly phosphorylated [16–18, 22, 23]. Some of the identified phosphorylation sites promote the assembly of the Myo2-Vac17-Vac8 complex, while other sites are required for the termination of vacuole transport. We reasoned that the discovery of regulatory sites in Vac17, and the related kinases, have the potential to reveal essential steps for the termination of vacuole transport.

We hypothesized that a vacuolar kinase may regulate vacuole transport. Yck3 is constitutively localized on the vacuole [24]. Moreover, Yck3-dependent phosphorylation of

some of its targets releases them from protein complexes on the vacuole membrane [25, 26]. These studies raised the possibility that Yck3 has a role in the disassembly of the Myo2-Vac17-Vac8 complex.

We tested and found that a *yck3* mutant results in the accumulation of Vac17-GFP and the vacuole at the bud tip and mother-bud neck, similar to a *dma1* mutant (Figure 1A). Since these two distinct phenotypes appear in a similar percentage of cells, we show representative images of both. Additionally, deletion of Yck3 results in elevated levels of endogenous Vac17, similar to the *dma1* mutant (Figure 1B). These studies strongly suggest that Yck3 has a role in the termination of vacuole transport. Although it was previously reported that Yck3 may have a role in the initiation of vacuole transport [27], we only observed a defect in the termination of vacuole transport in the strain backgrounds used in this study.

We then tested if Vps41 also has a role in the termination of vacuole transport. Vps41 is a subunit of the HOPS complex [28–32], and is required for fusion of endosomes with the vacuole, and vacuole-vacuole fusion [31–33]. Vps41 is also a downstream target of Yck3 [27, 34]. We found that the *vps41* and *yck3 vps41* mutants resulted in the accumulation of the vacuole and Vac17-GFP at the bud tip and mother-bud neck (Figure 1A), and also resulted in elevated levels of endogenous Vac17 (Figure 1B). These phenotypes are similar to those observed in the *yck3* and *dma1* mutants. Note that the *vps41* mutant has fragmented vacuoles due to the role of Vps41 in vacuole fusion [28–32]. These data indicate that both Yck3 and Vps41 have roles in the termination of vacuole transport.

In further support that Vps41 and Yck3 are required to release the vacuole from Myo2, the vacuole accumulates at the bud tip and mother-bud neck with Myo2-Venus in the *vps41*, *yck3*, and *yck3 vps41* mutants, similar to a *dma1* mutant (Figure S1A). Additionally, Vac17-GFP accumulates at the bud tip and mother-bud neck with mCherry-Myo2 in the *vps41*, *yck3*, or *yck3 vps41* mutants (Figure S1B). Together, these data support the hypothesis that Vps41 and Yck3 are required for the release of the vacuole from Myo2 and the subsequent degradation of Vac17.

The roles of Yck3 and Vps41 in the termination of vacuole transport are independent of the HOPS complex, CORVET complex, and AP-3 trafficking

Yck3 was previously shown to regulate Vps41 through phosphorylation [27, 34, 35]. A non-phosphorylatable mutant promotes the localization of Vps41 to the vacuole, while the phosphomimetic mutant displaces Vps41 from the vacuole [34]. We tested if these Vps41 mutants had defects in the termination of vacuole transport. However, they support the termination of vacuole transport and do not recapitulate the *vps41* mutant (Figure 2A). This raises the possibility that the roles of Yck3 and Vps41 in vacuole transport are separate from their roles in vacuole fusion. Two previous studies also suggested that Vps41 has functions independent of the HOPS complex [36, 37].

We tested if other HOPS subunits are required for the termination of vacuole transport. We found that deletion of Vps39, the other HOPS-specific subunit, did not result in the accumulation of Vac17-GFP at the bud tip or mother-bud neck (Figure 2B), and did not elevate Vac17 levels (Figure 2C). The four core HOPS subunits, Vps11, Vps16, Vps18, and

Vps33, are also found in the class C core vacuole/endosome tethering (CORVET) complex, another vesicle tethering complex [33, 38]. Loss of function of these subunits results in defects in the initiation of vacuole transport [39]. Thus, we only scored cells that inherited vacuoles. By microscopy, there was neither an accumulation of Vac17-GFP nor mis-localization of the vacuole in temperature sensitive mutants of Vps11, Vps16, Vps18, or Vps33 (Figure S2). These findings suggest novel roles of Vps41 and Yck3 that are independent of their known roles in HOPS.

Vps41 also has roles in adaptor protein-3 (AP-3) vesicle trafficking, which is required for the ALP pathway that traffics proteins to the vacuole [35, 40–42]. Vps41 may also form intermediate complexes with Vps3 [43], suggesting a link to CORVET specific subunits. Neither deletion of AP-3 components Apl5, Ap3, Apl6, and Apm3, nor deletion of CORVET specific subunits, Vps3 and Vps8, resulted in defects in the termination of vacuole transport (Figure S3). Thus, Vps41 and Yck3 likely act independently of HOPS, CORVET, and AP-3 and have uncharacterized roles in terminating vacuole transport.

The roles of Yck3 and Vps41 are independent of Vac17 ubiquitylation

Ubiquitylation of Vac17 is required for the degradation of Vac17 and the release of the vacuole from Myo2 [22, 23]. The ubiquitylation of Vac17 requires: 1) the phosphorylation of Vac17-T240, which leads to 2) the recruitment of inactive Dma1 to Vac17, 3) the vacuole is brought to the bud cortex where Cla4 phosphorylates Vac17-S222, which leads to 4) activation of Dma1 and the ubiquitylation of Vac17. Abolishing any of the steps prevents the ubiquitylation of Vac17 and results in defects in the termination of vacuole transport [22, 23].

We first tested if Yck3 and Vps41 are required for the recruitment of Dma1 to Vac17. We found that Dma1-GFP localizes to the leading edge of the vacuole in the *vps41* and *yck3* mutants, similar wild type (Figure 3A). Moreover, the phosphorylation of Vac17-T240, a prerequisite of Dma1 binding, occurs in wild type and the *yck3* mutant, but not the non-phosphorylatable *vac17-T240A* mutant (Figure 3B). Note that a *dma1 dma2* mutant was used to elevate Vac17 levels to facilitate detection by the phospho-specific antibody.

We then tested the localization and activity of Cla4. In small-budded cells, Cla4 is localized on the bud cortex [44]. After the vacuole contacts the cortex, a punctum of Cla4 localizes to the vacuole [44]. In small-budded *vps41* and *yck3* mutants, Cla4-GFP co-localizes with the vacuole, similar to wild type (Figure 3C). Additionally, Vac17-S222, the target of Cla4, is phosphorylated in wild type and the *yck3* mutant, but not in the non-phosphorylatable *vac17-S222A* mutant (Figure 3B). Thus, the localization of Dma1 and activity of Cla4 do not depend on Yck3 and Vps41 (Figure 3A–C).

Since Dma1 is recruited to Vac17 and Cla4 phosphorylates S222, we hypothesize that Vac17 is ubiquitylated in the *vps41* and *yck3* mutants. Indeed, Yck3 and Vps41 are not required for the ubiquitylation of Vac17 (Figure 3D). Previous hypotheses assumed that ubiquitylation was the last step prior to the degradation of Vac17. Our studies indicate that at least two independent, non-redundant pathways are required to dissociate the vacuole from Myo2 and degrade Vac17. Yck3 and Vps41 function independently of Cla4 and Dma1, and

ubiquitylation is independent of Vps41 and Yck3. These findings raise the possibility that Yck3 and Vps41 act in another manner to regulate the termination of vacuole transport.

Yck3 and Vps41 regulate the release of ubiquitylated Vac17 from the Myo2-Vac17-Vac8 complex

Since ubiquitylation alone is not sufficient to release Myo2 from the vacuole, we turned to a genetic approach to determine whether Yck3 and Vps41 function with or upstream of the proteasome for Vac17 degradation. We previously showed that loss of function proteasome mutants results in elevated levels of Vac17 [23]. However, the localization of Vac17 in these mutants was not determined.

We found that Vac17 is released from the vacuole in the *pre2-T76A* mutant (Figure 4A), the *pre1–1* mutant (Figure 4B), and the *pup1-K58E pup3-E151K* mutant (Figure 4C). Pup1, Pup3, Pre1, and Pre2 comprise Beta subunits of the 20S core particle of the proteasome [45, 46]. In each of the 20S proteasome mutants tested, Vac17-GFP appears in puncta that are not strictly on the vacuole or at the bud tip or mother-bud neck (Figure 4A–C). These findings suggest that Vac17 is released from the vacuole, and likely from the Myo2-Vac17-Vac8 complex, before Vac17 is degraded by the proteasome.

Next, we performed epistasis experiments where the phenotype of the double mutant indicates the upstream step of a pathway. Strikingly, the proteasome mutant combined with deletion of either Yck3 or Vps41 phenocopies the single *yck3* or *vps41* mutants, where Vac17 is trapped in the Myo2-Vac17-Vac8 complex and accumulates with the vacuole at the bud tip or mother-bud neck (Figure 4C). These findings show that Yck3 and Vps41 act upstream of the proteasome.

The observation that Vac17 is released from the vacuole raised the question of whether Myo2 and/or Vac8 are also delivered to the proteasome. However, Myo2 and Vac8 levels are not altered in the *pup1-K58E pup3-E151K* mutant alone or in combination with the *yck3* or *vps41* mutants by western blot (Figure 4D). This is in contrast to Vac17-GFP, which is elevated in the *pup1-K58E pup3-E151K* and/or *yck3* or *vps41* mutants compared to wild type (Figure 4D). Additionally, Myo2-Venus remains at sites of polarized growth (Figure S4A) and Vac8-mCherry remains on the vacuole (Figure S4B) in the *pup1-K58E pup3-E151K* mutant. CMAC, a small molecule that stains the lumen of the vacuole [47, 48], was used as a vacuole marker when we tested Vac8 localization. Overall, these data indicate that Yck3 and Vps41 act upstream of the proteasome to dissociate ubiquitylated Vac17 from the Myo2-Vac17-Vac8 complex on the vacuole, which releases the vacuole from Myo2 and allows for the degradation of ubiquitylated Vac17.

The AAA-ATPases Cdc48/p97, Vps4, and Sec18/NSF do not extract Vac17 from the complex

Several AAA-ATPases have been shown to extract proteins from membranes or protein complexes to facilitate their degradation. Cdc48/p97 extracts endoplasmic reticulum membrane proteins destined for degradation [49, 50]. Vps4 aids in the disruption of ESCRT-III complex on endosomes [51]. Sec18/NSF is AAA-ATPase that disassembles SNARE complexes at multiple cellular locations, including the vacuole [52–54]. However, the

cdc48–3 temperature sensitive mutant, (Figure S5A), a *vps4* mutant (Figure S5B), and a *sec18-DAmP* mutant (Figure S5C) did not have defects in the termination of vacuole transport. In budding yeast, there are about fifty AAA ATPases [55], with at least ten confirmed as unfolding ATPases [56]. It is possible that a currently unidentified AAA-ATPase, or a different mechanism, facilitates the release of Vac17 from the Myo2-Vac17-Vac8 complex.

Yck3 and Vps41 bind and are required for the phosphorylation of Vac17

Our data suggest that Yck3 and Vps41 target Vac17. Consequently, we tested if Yck3 can bind to Vac17. Since Yck3 function was not required for Cla4 or Dma1 regulation of Vac17, we also tested if Yck3 could bind the *vac17- PEST* mutant, which is missing the sites of Dma1 binding and Cla4 phosphorylation (Figure 5A). Recombinant GST-Yck3 (2–516) immobilized on beads binds to Vac17-TAP and Vac17- PEST-TAP from yeast lysates (Figure S6A). This indicates that Yck3 may bind to Vac17 and that this interaction does not require the Vac17-PEST sequence. Interestingly, this interaction does not require Vps41 (Figure S6A). We also found that recombinant His-Vps41 (124–992) from *C. thermophilium* binds to Vac17-TAP and Vac17- PEST-TAP from yeast lysates (Figure S6B). This interaction also occurred in a *yck3* mutant (Figure S6B). Note that these interactions with Vac17 may be indirect and facilitated by an unknown protein present in the yeast lysates. These data demonstrate that both Yck3 and Vps41 bind directly or indirectly to Vac17 outside of the PEST sequence.

Since Yck3 is a kinase, and the *yck3* and *vps41* mutants have similar phenotypes, we hypothesized that Yck3 and Vps41 regulate the phosphorylation of Vac17- PEST. Using a gel shift assay, we found that Yck3 and Vps41 -dependent phosphorylation occurred in the *vac17- PEST* mutant. The addition of phosphatase collapses the higher mobility band in Vac17- PEST-GFP, which is rescued by phosphatase inhibitors (Figure 5B). In the *yck3* and *vps41* mutants, addition of phosphatase does not result in any change in gel mobility, suggesting that shift in Vac17- PEST-GFP is due to Yck3 and Vps41 -dependent phosphorylation (Figure 5B). Previously known regulators, Cla4 and Dma1, regulate or bind Vac17 via the PEST sequence. That Yck3 and Vps41 regulate Vac17 outside of its PEST sequence suggests a new mode of regulation in the termination of vacuole transport.

We also tested if Yck3 and Vps41 –dependent phosphorylation requires an intact Myo2-Vac17-Vac8 complex. The *myo2-D1297N* mutant is unable to bind to Vac17, and Vac17 is bound to Vac8 on vacuoles that remain in the mother cell [57]. We found in a gel shift assay that Vac17- PEST-GFP is not phosphorylated in the *myo2-D1297N* mutant (Figure 5C). Next, we tested a *vac8* mutant in which Vac17 is bound to Myo2 and brought to the bud, but is not associated with the vacuole [18]. We found that Vac17- PEST-GFP is not phosphorylated in a *vac8* mutant (Figure 5D). These data suggest that Vac17 needs to be on the vacuole in the bud and/or in a complex with Myo2 and Vac8 to be phosphorylated by Yck3 and Vps41. Yck3 and Vps41 might regulate the phosphorylation of Vac17 after the Myo2-Vac17-Vac8 complex is formed, or if Vac17 is in the bud and on the vacuole.

We also used a gel shift assay to determine if Dma1 is required for the Yck3 -dependent phosphorylation of Vac17. In a *dma1 dma2 yck3* mutant, Vac17- PEST-GFP has

increased mobility compared to a *dma1 dma2* mutant (Figure 5E), indicating that Dma1/ Dma2 are not required for Yck3-dependent phosphorylation of Vac17. Of note, Vac17-PEST-GFP appears to be at lower levels in a *dma1 dma2* mutant compared to wild type or *yck3* backgrounds (Figure 5E). This may be due to compensatory mechanisms that lower Vac17-PEST levels in the *dma1 dma2* mutant. Consistent with previous data, these findings suggest that Dma1-dependent ubiquitylation and Yck3 and Vps41-dependent phosphorylation occur through independent pathways.

Yck3 and Vps41 phosphorylate Vac17 in the Myo2 binding domain

To determine Vps41 and Yck3-dependent phosphosites on Vac17, we performed Stable Isotope Labeling by Amino acids in Cell culture (SILAC) mass spectroscopy. We identified multiple sites in Vac17-PEST whose phosphorylation status is changed in the *vps41* mutant (Table S1). Interestingly, four of the phosphosites reside in the Myo2 binding domain: S127, S128, S131, and T149. One of these sites, S131, was also reduced in the *yck3* mutant (Table S2).

We determined whether these sites are required for the termination of vacuole transport by testing the corresponding non-phosphorylatable alanine mutations. The *vac17–4A* mutant had a defect in the termination of vacuole transport similar to the *yck3* mutant, as assessed by microscopy (Figure 6A) and western blot (Figure 6B). Note that Vac17-T149 was identified as one of four Cdk1 sites important for the initiation of vacuole transport [18]. However, the *vac17-T149A* mutant alone did not have defects in vacuole transport (Figure 6A). These data suggest that these residues are required for the release of the vacuole from Myo2 and the degradation of Vac17.

We then tested the putative phosphomimetic mutant, *vac17–4E.* This mutant was not defective in the release of Myo2 from the vacuole and did not elevate levels of Vac17 (Figure 6 C–D, Figure S7A–D). Rather, the *vac17–4E* mutant acted like wild type, suggesting that phosphorylation of these residues is required for the termination of vacuole transport.

We further tested the *vac17–4A* and *vac17–4E* mutants in combination with the *pup1-K58E pup3-E151K* proteasome mutant. In the *vac17–4A pup1-K58E pup3-E151K* mutant, Vac17–4A-GFP accumulated at the bud tip or mother-bud neck instead of in puncta (Figure 6C). Moreover, compared to wild type, the *vac17–4A* mutant had elevated levels of Vac17, and the *vac17–4A pup1-K58E pup3-E151K* mutant elevated Vac17 to levels greater than the *pup1-K58E pup3-E151K* mutant alone (Figure 6D). Since the phenotype of *vac17–4A pup1-K58E pup3-E151K* mutant is the same as the *vac17–4A-GFP* mutant alone, this further suggests that these phosphosites are important for the release of Vac17 from the Myo2-Vac17-Vac8 complex. Conversely, when expressed in a *pup1-K58E pup3-E151K* mutant, Vac17–4E-GFP behaved similarly to a proteasome mutant alone and accumulated in aberrant puncta (Figure 6C). Together these findings suggest that phosphorylation of Vac17-S127, S128, S131, and T149 are required to release Vac17 from the Myo2-Vac17-Vac8 complex.

We also tested whether the *vac-4A* or *vac-4E* mutant had altered binding to Myo2. While we saw a modest trend of increased association of Myo2 with Vac17–4A (1–355) and decreased association with Vac17–4E (1–355), these differences were not statistically significant (Figure 6E). Additionally, the *vac17–4E* mutant did not suppress the *yck3Δ* mutant (Figure S7A–B) or *vps41Δ* mutant (Figure S7C–D). This suggests that phosphorylation of these four sites are necessary but not sufficient for the release of Vac17 from the Myo2-Vac17-Vac8 complex. There are likely additional phosphorylation sites on Vac17 or phosphorylation of other members of the complex, and/or other proteins that act in the removal of Vac17 from the Myo2-Vac17-Vac8 complex.

Notably, while Vps41 plays a role in the phosphorylation of all four residues, deletion of Yck3 did not result in a loss of phosphorylation of Vac17 -S127, -S128 or T149, but exhibited a decrease in phosphorylation of Vac17-S131 (Table S2). This site matches the casein kinase I consensus sites, SxxS, or where the target residue is 1–3 amino acids downstream of acidic [58–60] or primed residues (residues that have already been phosphorylated) [60–62]. Thus, it is likely that Vps41 is regulating additional kinases, such as a priming kinase, to phosphorylate these sites. Overall, Vps41 promotes the phosphorylation of the Myo2 binding domain of Vac17 likely via additional kinase(s) and perhaps as an upstream regulator of Yck3.

Additional phosphorylation sites adjacent to the Vac8 binding domain, Vac17 -S269, S272, and S275, were also identified (Table S1, Table S2), and these sites were heavily dependent on Yck3. However, the non-phosphorylatable alanine mutant, *vac17-S269A-S272A-S275A*, did not have defects in the termination of vacuole transport or degradation of Vac17 (Figure S7E–F). Note that the *vac17-S269A-S272A-S275A* mutant exhibited a faster mobility on SDS-PAGE compared with wild type Vac17, suggesting that these are bona fide phosphorylation sites. These data further support the hypothesis that there are additional steps required to release Vac17 from the Myo2-Vac17-Vac8 complex.

Overall, these data suggest that Vps41 and Yck3 are each required to regulate the phosphorylation of Vac17 at the interface between Vac17 and Myo2, and for the dissociation Vac17 from the motor-adaptor complex. Previous studies of Vac17 degradation indicated that the Vac17-PEST sequence is required for the ubiquitylation of Vac17 [17, 22, 23]. Our new studies indicate that Yck3 and Vps41 regulate binding between Vac17 and Myo2 to release ubiquitylated Vac17 from the Myo2-Vac17-Vac8 complex and terminate vacuole transport.

Discussion

Our data reveal that release of the vacuole from Myo2 requires two pathways that act on the adaptor, Vac17. In one pathway, the bud-localized kinase, Cla4, phosphorylates Vac17, which facilitates the Dma1-dependent ubiquitylation of Vac17. In the other pathway, Yck3 and Vps41 regulate the phosphorylation of Vac17 in its Myo2 binding domain, and potentially other regions. Both ubiquitylation and Yck3 and Vps41-dependent regulation are required to release Vac17 from the Myo2-Vac17-Vac8 complex. Vac17 is then degraded by the proteasome (Figure 7). In mutants where Yck3 and Vps41 are present, but ubiquitylation

of Vac17 is defective, Vac17 is not released from the complex. Similarly, in mutants where Vac17 is ubiquitylated but Yck3 and/or Vps41 are absent, Vac17 is not released from the complex. However, in loss of function proteasome mutants, where both ubiquitylation and Yck3 and Vps41 -dependent regulation occur, Vac17 is released from the vacuole, but not degraded. Note that Vac17 levels are elevated in the proteasome mutant where the Myo2-Vac17-Vac8 complex is disassembled, suggesting that elevated Vac17 alone does stabilize the complex. Together, these data support a model where both ubiquitylation and a Yck3 and Vps41 -dependent pathway act in parallel to dissociate the Myo2-Vac17-Vac8 complex, and lead to the degradation of Vac17 (Figure 7). Yck3 and Vps41 may function in different steps of this pathway, as a fully detailed molecular mechanism remains unclear.

Our data strongly suggest that Vps41 acts in the release of Vac17 via regulation of kinase(s) that phosphorylate Vac17-S127, S128, S131, and T149, residues within the Myo2 binding region. Yck3 is one candidate kinase, which plays a role in the phosphorylation of Vac17-S131. An unidentified kinase may be responsible for phosphorylation of the other sites. It is possible that Vps41 is regulating multiple steps in this pathway or acts upstream of several kinases including Yck3.

Given the strong phenotype of *yck3*, it is likely that additional Yck3 sites within Vac17, Vac8, and/or Myo2, are not yet identified. While Yck3 and Vps41 are required for the phosphorylation of three sites in the Vac8 binding region of Vac17, the function of these sites are unknown and additional regulatory steps may be required. Moreover, Yck3 and/or Vps41 may regulate the phosphorylation of residues within the Vac17-PEST sequence. The phosphorylation of these potentially unidentified residues may depend on the ubiquitylation of Vac17.

The requirement for parallel pathways suggests that an additional factor may act as a coincidence detector that establishes that both events have occurred and then allows dissociation of the complex. Such a factor may recruit machinery that physically releases Vac17, such as a AAA-ATPase. Alternatively, Yck3 and Vps41–dependent phosphorylation may change Vac17 conformation and/or work with the proteasome to dissociate Vac17 from the complex.

A question raised by these studies is why release of Myo2 from the vacuole involves multiple mechanisms. Myo2 transports the vacuole, a relatively large organelle, through the crowded cytoplasm and the narrow mother-bud neck. It is likely that Myo2, Vac17, and Vac8 are tightly associated with each other in the complex to prevent premature release of the vacuole. The regulated release of Myo2 from the vacuole is likely critical for Myo2 attachment to its essential cargo, secretory vesicles, which seal the membrane at the mother-bud neck during cytokinesis [63]. Degradation of free Vac17 may be required to prevent untimely reassembly of the complex. It is also possible that additional cues regulate the Yck3 and Vps41-dependent phosphorylation of Vac17 to coordinate vacuole delivery with other cellular processes, such as vacuole membrane fusion. Overall, these studies reveal a mechanism of how a cargo is released from myosin V.

STAR Methods

Resource Availability

Lead Contact—Further information and requests for resources and reagents should be directed to and will be fulfilled by the Lead Contact, Lois S. Weisman (lweisman@umich.edu)

Materials Availability—Yeast strains, plasmids, and antibodies generated in this study are available upon request.

Data and Code Availability—This study did not generate or analyze datasets or code.

Experimental Model and Subject Details

Yeast strains, plasmids, and media—Yeast strains and plasmids are listed in Key Resources Table. Yeast cultures were grown in yeast extract peptone dextrose (YEPD) containing 1% yeast extract, 2% peptone and 2% dextrose or synthetic complete (SC) media lacking the indicated amino acid (s) at 24°C unless specified.

Method Details

Western Blot analysis—2–10 OD's of cells were lysed in ice-cold 1 mL 0.2 M NaOH/ 0.2% β-mercaptoethanol and incubated on ice for 10 min. 100 μL trichloroacetic acid (TCA) was added to the lysates and incubated on ice for 5 min. Precipitated proteins were harvested via centrifugation at 13,000 rpm for 5 min. Pellets were resuspended in 100 μL 2X SDS sample buffer (0.12M Tris-HCl (pH 6.8), 19% Glycerol, 0.15 mM Bromophenol Blue, 3.8% SDS, 0.05% β-mercaptoethanol). 20 μL of 1 M Tris base (pH 11) was then added and the samples were heated at 75°C for 10 min. Protein samples were loaded on 9% SDS PAGE gels made with Acrylamide/bis (30% 37.5:1; Bio-Rad) and run at 70–100V. Proteins were transferred onto nitrocellulose membrane at 35V for 19 hours. Membranes were blocked in milk before incubation in the primary antibodies indicated. Membranes were washed 3 times, 10 min each in TBST, incubated in secondary antibodies, washed again, and developed with ECL or ECL prime. For immunoblot analyses, mouse anti-GFP (1:1,000; Roche), rabbit anti-TAP (1:1,000; Invitrogen), mouse anti-Pgk1 (1:10,000; Invitrogen), sheep anti-Vac17 (1:1,000; custom made, Twenty First Century Biochemicals), rabbit anti-phosphoThr240 (1:2,500; custom made, 21st Century Biochemicals) and rabbit anti-phosphoSer222 (1:2,500; custom made, 21st Century Biochemicals) antibodies were used (see Antibody Preparation). Pgk1 was used as a loading control for whole cell lysates. All blots shown are representative of n=3. Molecular mass is shown in kilodaltons (kDa).

Immunoprecipitation experiments—Cells were lysed and proteins were precipitated as described above. Precipitated proteins were washed with acetone, dried, and resuspended in 200 μL urea buffer (6 M urea, 1% SDS, 50 mM Tris-HCl pH 7.5), and heated at 75°C for 10 min. 1.8 ml TWIP buffer (50 mM Tris-HCl pH 7.5, 150 mM NaCl, 0.5% Tween-20, 0.1 mM EDTA) containing 1 mM Na3VO4 and 1X protease inhibitor cocktail (Sigma) was added to the resuspended protein and centrifuged. 4 μg of mouse anti-GFP antibodies (Roche) were added to the supernatant and incubated with agitation at 4°C, overnight. Immune complexes

were harvested via the addition of protein G beads, which were subsequently collected via centrifugation and washed with TWIP buffer. Bound proteins were analyzed via immunoblot.

In vivo ubiquitylation experiments—To detect ubiquitylated Vac17, pVT102U-Vac17-GFP was transformed into *vac17Δ*, *dma1Δ dma2Δ vac17Δ*, *yck3Δ vac17Δ* or *vps41Δ vac17Δ* mutant strains. pVT102U-Vac17 was transformed into *vac17Δ* as a no-GFP control. A plasmid encoding Myc-Ub driven by a CUP1 promoter was co-transformed into the same strains. Myc-Ub expression was induced with 100 μM CuCl2. GFP fusion proteins were immunoprecipitated as described above and analyzed via immunoblot using rabbit anti-GFP (Abcam), and rabbit anti-Myc antibodies (1:2,000; Cell Signaling).

Microscopy—To visualize vacuoles, cells were labeled with either (1) 12 μg FM4–64 (SynaptoRed™ C2, Sigma-Aldrich) in 250 μL media for 1 hour, then washed twice and grown in 5 ml fresh media for one doubling time (2–3 hours), or (2) 100 μM 7-aminochloromethylcoumarin (CellTracker Blue CMAC Dye, Thermo Fisher) 30 minutes, then washed in fresh media and imaged. Live cell images were obtained on a DeltaVision Restoration system (Applied Precision) using an inverted epifluorescence microscope (IX-71; Olympus) with a charge-coupled device camera (Cool-SNAP HQ; Photometrics) and processed in Photoshop and ImageJ. DIC indicates differential interference contrast. Scale bars in representative images are 5 μm.

Alpha Factor Cell Synchronization—100 ml of cells (OD = 0.2–0.4) were incubated in 2.5 μM alpha-factor (Zymo Research) for 2–3 hours until 80% of cells were arrested in G1. Cells were washed in fresh media twice to remove alpha-factor. 1mL aliquots were collected every 10 minutes.

GST Tag Binding Assay—GST and GST-Yck3 were expressed in Rosetta (DE3) pLySS cells (Novagen) via induction with 0.1 mM IPTG at 30°C for 5 hours. Cells were resuspended in GST lysis buffer (50mM Tris pH 7.5, 150mM NaCl, 5mM EDTA, 1 mM Pefabloc [Sigma-Aldrich], and cOmplete EDTA-free protease inhibitor cocktail [Roche]) and lysed via sonication. Lysates were clarified via centrifugation at 20,000 g for 30 min at 4°C and incubated with glutathione beads at 4°C with agitation. Immobilized proteins were washed once with GST lysis buffer. Yeast cells grown in yeast extract peptone dextrose at 24°C were resuspended in yeast lysis buffer (125mM NaCl, 50mM NaPO$_4$ pH 7.4, 10% glycerol, 2mM MgCl$_2$, 0.5% octyl glucosidase, 1mM DTT, 1× protease inhibitor cocktail (Sigma-Aldrich), and cOmplete EDTA-free protease inhibitor cocktail (Roche)) and lysed with glass beads. GST- and GST-Yck3 bound beads were incubated with clarified yeast cell extracts for 1 hr at 4°C with agitation. Beads were then washed twice with yeast wash buffer (50mM HEPES-KOH pH 7.4, 150mM KCl, 1mM EDTA, 10% glycerol). Bound proteins were analyzed via SDS-PAGE, Gelcode Blue Stain Reagent (Thermo Scientific), and immunoblotting. For input (6.25%), 20 μL lysate was resuspended in 20 μl sample buffer, and 5 μL was loaded into the gel.

HIS Tag Binding Assay—His and His-Vps41 were expressed in C43 (DE3) cells (Lucigen) via induction with 0.5mM IPTG at 30°C for 3 hours. Cells were resuspended in

Vps41 lysis buffer (10mM HEPES pH 7.4, 350mM NaCl, 2mM MgCl2, 5% glycerol, 50mM imidazole, 100μM PMSF, 5mM β-mercaptoethanol) and lysed via sonication. Lysates were clarified via centrifugation at 20,000 g for 30 min at 4°C and incubated with Ni-NTA beads at 4°C with agitation for 1 hour. Immobilized proteins were washed twice with Vps41 lysis buffer. Yeast cells grown in yeast extract peptone dextrose at 24°C were resuspended in yeast lysis buffer (125mM NaCl, 50mM NaPO$_4$ pH 7.4, 10% glycerol, 2mM MgCl$_2$, 0.5% octyl glucosidase, 1mM DTT, 1× protease inhibitor cocktail (Sigma-Aldrich), and cOmplete EDTA-free protease inhibitor cocktail (Roche)) and lysed with glass beads. His- and His-Vps41 bound beads were incubated with clarified yeast cell extracts for 1 hr at 4°C with agitation. Beads were then washed twice with yeast wash buffer (50mM HEPES-KOH pH 7.4, 150mM KCl, 1mM EDTA, 10% glycerol). Bound proteins were analyzed via SDS-PAGE, Gelcode Blue Stain Reagent (Thermo Scientific), and immunoblotting. For input (6.25%), 20 μL lysate was resuspended in 20 μL sample buffer, and 5 μL was loaded into the gel.

Lambda Phosphatase Treatment—Log phase cells (20 OD600 units) were suspended in 1 mL ice cold 0.2M NaOH, 0.2% b-mercaptoethanol (v/v), and incubated on ice for 10 min. 100μL trichloroacetic acid (TCA) was added and incubated on ice 10 min. Protein pellets were washed three times with acetone and air dried. The pellets were resuspended in 200 μL urea breaking buffer (6M Urea, 1% SDS, 50mM Tris-HCl pH 7.5) and heated at 75°C. 1800 μL of TWIP (50mM Tris-HCl pH 7.5, 150mM NaCl, 0.5% Tween-20, 1× protease inhibitor cocktail (Sigma-Aldrich), NaVO4, 1mM PMSF) was added and the lysate was spun 5000 rpm 5min. 4μg/μL of mouse-anti-GFP was added to the supernatant and incubated 1 hr at 4°C with agitation. Protein G beads were added and incubated 1 hr at 4°C with agitation. Beads were washed in TWIP and resuspended in 50 μL master mix (40μL water + 5μL 1 × λ-phosphatase buffer + 1× protease inhibitor cocktail (Sigma-Aldrich) + 5μL 10 mM MnCl2). Either water, λ-phosphatase (400 U; New England Biolabs, Inc.), or λ-phosphatase plus phosphatase inhibitors (100 mM NaF, 10 mM Na3VO4, 50 mM EDTA, 20 mM β-glycerophosphate, and 20 mM sodium pyrophosphate) were added to the reaction. Phosphatase reactions were incubated 1 hr at 30°C with agitation. Reactions were stopped with addition of 2x sample buffer (0.12M Tris-HCl (pH 6.8), 19% Glycerol, 0.15 mM Bromophenol Blue, 3.8% SDS, 0.05% β-mercaptoethanol). The resultant samples were subjected to immunoblot analysis.

SILAC—LWY18795, LWY18802, and LWY18813 were co-transformed with pVT102u-Vac17- PEST-6xHis-TEV-3xFLAG and pRS413-Myo2-D1297N. Note that the pRS413-Myo2-D1297N mutant was included to improve viability of the yeast, which may be negatively affected by over expression of Vac17 mutants that occupy Myo2 and prevent Myo2 from performing essential functions. SILAC-based mass spectrometry for quantitation and mapping of Vac17 phosphosites was performed as previously described [64, 65] with slight modification. Briefly, equal amount of light wildtype) and heavy (yck3 or vps41, as indicated) cells expressing exogenous Vac17- PEST-FLAG were harvested from mid-log phase and disrupted by bead beating using ice-cold lysis buffer (50 mM Tris-HCl, pH 7.5, 150 mM NaCl, 5 mM EDTA, 0.2% NP-40, 10 mM iodoacetamide, 1X EDTA-free protease inhibitor cocktail (Roche), 1mM phenylmethylsulfonyl fluoride, 20 μM MG132, 1X

PhosStop (Roche), 10 mM NaF, 20 mM BGP, and 2 mM Na_3VO_4). Lysate was clarified by centrifugation at 21,000 x g for 10 min at 4°C and supernatant was transferred into a new tube and diluted with threefold volume of ice-cold TBS (50 mM Tris-HCl, pH7.5, 150 mM NaCl). Vac17- PEST-FLAG in 12-ml diluted lysate was enriched by incubation with 50 μl of EZview anti-FLAG M2 resin slurry (Sigma) for 2 h at 4°C with rotation. The resin was washed three times with cold TBS and incubated with 90μl elution buffer (100 mM Tris-HCl, pH 8.0, 1% SDS) at 98°C for 5 min. Collected eluate was reduced with 10mM DTT, alkylated with 20mM iodoacetamide, and precipitated with 300 μl PPT solution (50% acetone, 49.9% ethanol, and 0.1% acetic acid). Light and heavy protein pellets were dissolved with Urea-Tris solution (8 M urea, 50 mM Tris-HCl, pH 8.0). Heavy and light samples were combined, diluted fourfold with water, and digested with 1μg MS-grade trypsin (Gold, Promega) by overnight incubation at 37°C. Phosphopeptides were enriched by immobilized metal affinity chromatography (IMAC) using Fe(III)-nitrilotriacetic acid resin as previously described [66], redissolved in 0.1% trifluoroacetic acid, and loaded onto a Q-Exactive mass spectrometer (Thermo Scientific). Resolved spectra were searched using MaxQuant (ver. 1.6.5.0) and chromatograms were visualized using Skyline (ver. 19.1.0.193, MacCoss Lab).

Quantification and Statistical Analysis

Statistical Analysis—Statistical tests (indicated in the Figure Legends) were conducted using PRISM (ver 8.0.2(263), GraphPad). p values are as indicated, ns = not significant. For each condition, measurements were taken from at least three independent yeast cultures (n=3) with 40 cells per n. Error bars indicate Standard Error of Mean (SEM).

Supplementary Material

Refer to Web version on PubMed Central for supplementary material.

Acknowledgements

References

1. Hill Kent L., N.L.C., and Weisman Lois S. (1996). Actin and Myosin Function in Directed Vacuole Movement during Cell Division in Saccharomyces cerevisiae. J Cell Biol 135, 1535–1549. [PubMed: 8978821]

2. Catlett Natalie L., a.L.S.W. (1998). The terminal tail region of a yeast myosin-V mediates its attachment to vacuole membranes and sites of polarized growth. Proc Natl Acad Sci USA 95, 14799–14804. [PubMed: 9843969]

3. Simon VR, Swayne TC, and Pon LA (1995). Actin-dependent mitochondrial motility in mitotic yeast and cell-free systems: identification of a motor activity on the mitochondrial surface. J Cell Biol 130, 345–354. [PubMed: 7615636]

4. Hoepfner D, van den Berg M, Philippsen P, Tabak HF, and Hettema EH (2001). A role for Vps1p, actin, and the Myo2p motor in peroxisome abundance and inheritance in Saccharomyces cerevisiae. J Cell Biol 155, 979–990. [PubMed: 11733545]

5. Pruyne DW, Schott DH, and Bretscher A (1998). Tropomyosin-containing actin cables direct the Myo2p-dependent polarized delivery of secretory vesicles in budding yeast. J Cell Biol 143, 1931–1945. [PubMed: 9864365]

6. Arai S, Noda Y, Kainuma S, Wada I, and Yoda K (2008). Ypt11 functions in bud-directed transport of the Golgi by linking Myo2 to the coatomer subunit Ret2. Curr Biol 18, 987–991. [PubMed: 18595704]

7. Hwang E, Kusch J, Barral Y, and Huffaker TC (2003). Spindle orientation in Saccharomyces cerevisiae depends on the transport of microtubule ends along polarized actin cables. J Cell Biol 161, 483–488. [PubMed: 12743102]

8. Lee L, Tirnauer JS, Li J, Schuyler SC, Liu JY, and Pellman D (2000). Positioning of the mitotic spindle by a cortical-microtubule capture mechanism. Science 287, 2260–2262. [PubMed: 10731147]

9. Liakopoulos D, Kusch J, Grava S, Vogel J, and Barral Y (2003). Asymmetric loading of Kar9 onto spindle poles and microtubules ensures proper spindle alignment. Cell 112, 561–574. [PubMed: 12600318]

10. Miller RK, Cheng SC, and Rose MD (2000). Bim1p/Yeb1p mediates the Kar9p-dependent cortical attachment of cytoplasmic microtubules. Mol Biol Cell 11, 2949–2959. [PubMed: 10982392]

11. Yin H, Pruyne D, Huffaker TC, and Bretscher A (2000). Myosin V orientates the mitotic spindle in yeast. Nature 406, 1013–1015. [PubMed: 10984058]

12. Knoblach B, and Rachubinski RA (2014). Transport and Retention Mechanisms Govern Lipid Droplet Inheritance in Saccharomyces cerevisiae. Traffic.

13. Knoblach B, and Rachubinski RA (2016). How peroxisomes partition between cells. A story of yeast, mammals and filamentous fungi. Current opinion in cell biology 41, 73–80. [PubMed: 27128775]

14. Weisman LS (2006). Organelles on the move: insights from yeast vacuole inheritance. Nature Reviews Molecular Cell Biology 7, 251–251.

15. Westermann B (2014). Mitochondrial inheritance in yeast. Biochim Biophys Acta 1837, 1039–1046. [PubMed: 24183694]

16. Ishikawa K, Catlett NL, Novak JL, Tang F, Nau JJ, and Weisman LS (2003). Identification of an organelle-specific myosin V receptor. J Cell Biol 160, 887–897. [PubMed: 12642614]

17. Tang F, Kauffman EJ, Novak JL, Nau JJ, Catlett NL, and Weisman LS (2003). Regulated degradation of a class V myosin receptor directs movement of the yeast vacuole. Nature 422, 87–92. [PubMed: 12594460]

18. Peng Y, and Weisman LS (2008). The cyclin-dependent kinase Cdk1 directly regulates vacuole inheritance. Dev Cell 15, 478–485. [PubMed: 18804442]

19. Wang Yong-Xu, N.L.C., and Lois S Weisman (1998). Vac8p, a Vacuolar Protein with Armadillo Repeats, Functions in both Vacuole Inheritance and Protein Targeting from the Cytoplasm to Vacuole. J Cell Biol 140, 1063–1074. [PubMed: 9490720]

20. Tang F, Peng Y, Nau JJ, Kauffman EJ, and Weisman LS (2006). Vac8p, an armadillo repeat protein, coordinates vacuole inheritance with multiple vacuolar processes. Traffic 7, 1368–1377. [PubMed: 16824055]

21. Wang YX, Kauffman EJ, Duex JE, and Weisman LS (2001). Fusion of docked membranes requires the armadillo repeat protein Vac8p. J Biol Chem 276, 35133–35140. [PubMed: 11441010]

22. Yau RG, Wong S, and Weisman LS (2017). Spatial regulation of organelle release from myosin V transport by p21-activated kinases. J Cell Biol 216, 1557–1566. [PubMed: 28495836]

23. Yau RG, Peng Y, Valiathan RR, Birkeland SR, Wilson TE, and Weisman LS (2014). Release from myosin V via regulated recruitment of an E3 ubiquitin ligase controls organelle localization. Dev Cell 28, 520–533. [PubMed: 24636257]

24. Sun B, Chen L, Cao W, Roth AF, and Davis NG (2004). The yeast casein kinase Yck3p is palmitoylated, then sorted to the vacuolar membrane with AP-3-dependent recognition of a YXXPhi adaptin sorting signal. Mol Biol Cell 15, 1397–1406. [PubMed: 14668479]

25. Hickey CM, Stroupe C, and Wickner W (2009). The major role of the Rab Ypt7p in vacuole fusion is supporting HOPS membrane association. J Biol Chem 284, 16118–16125. [PubMed: 19386605]

26. Lawrence G, Brown CC, Flood BA, Karunakaran S, Cabrera M, Nordmann M, Ungermann C, and Fratti RA (2014). Dynamic association of the PI3P-interacting Mon1-Ccz1 GEF with vacuoles is controlled through its phosphorylation by the type 1 casein kinase Yck3. Mol Biol Cell 25, 1608–1619. [PubMed: 24623720]

27. LaGrassa TJ, and Ungermann C (2005). The vacuolar kinase Yck3 maintains organelle fragmentation by regulating the HOPS tethering complex. J Cell Biol 168, 401–414. [PubMed: 15684030]

28. Wada Y, Ohsumi Y, and Anraku Y (1992). Genes for directing vacuolar morphogenesis in Saccharomyces cerevisiae. I. Isolation and characterization of two classes of vam mutants. J Biol Chem 267, 18665–18670. [PubMed: 1526998]

29. Nakamura N, Hirata A, Ohsumi Y, and Wada Y (1997). Vam2/Vps41p and Vam6/Vps39p are components of a protein complex on the vacuolar membranes and involved in the vacuolar assembly in the yeast Saccharomyces cerevisiae. J Biol Chem 272, 11344–11349. [PubMed: 9111041]

30. Radisky DC, Snyder WB, Emr SD, and Kaplan J (1997). Characterization of VPS41, a gene required for vacuolar trafficking and high-affinity iron transport in yeast. Proceedings of the National Academy of Sciences of the United States of America 94, 5662–5666. [PubMed: 9159129]

31. Ungermann C, Price A, and Wickner W (2000). A new role for a SNARE protein as a regulator of the Ypt7/Rab-dependent stage of docking. Proceedings of the National Academy of Sciences of the United States of America 97, 8889–8891. [PubMed: 10908678]

32. Seals DF, Eitzen G, Margolis N, Wickner WT, and Price A (2000). A Ypt/Rab effector complex containing the Sec1 homolog Vps33p is required for homotypic vacuole fusion. Proceedings of the National Academy of Sciences of the United States of America 97, 9402–9407. [PubMed: 10944212]

33. van der Beek J, Jonker C, van der Welle R, Liv N, and Klumperman J (2019). CORVET, CHEVI and HOPS - multisubunit tethers of the endo-lysosomal system in health and disease. Journal of cell science 132.

34. Cabrera M, Ostrowicz CW, Mari M, LaGrassa TJ, Reggiori F, and Ungermann C (2009). Vps41 phosphorylation and the Rab Ypt7 control the targeting of the HOPS complex to endosome-vacuole fusion sites. Mol Biol Cell 20, 1937–1948. [PubMed: 19193765]

35. Cabrera M, Langemeyer L, Mari M, Rethmeier R, Orban I, Perz A, Brocker C, Griffith J, Klose D, Steinhoff HJ, et al. (2010). Phosphorylation of a membrane curvature-sensing motif switches function of the HOPS subunit Vps41 in membrane tethering. J Cell Biol 191, 845–859. [PubMed: 21079247]

36. Asensio CS, Sirkis DW, Maas JW Jr., Egami K, To TL, Brodsky FM, Shu X, Cheng Y, and Edwards RH (2013). Self-assembly of VPS41 promotes sorting required for biogenesis of the regulated secretory pathway. Dev Cell 27, 425–437. [PubMed: 24210660]

37. Pols MS, van Meel E, Oorschot V, ten Brink C, Fukuda M, Swetha MG, Mayor S, and Klumperman J (2013). hVps41 and VAMP7 function in direct TGN to late endosome transport of lysosomal membrane proteins. Nature communications 4, 1361.

38. Peterson MR, and Emr SD (2001). The class C Vps complex functions at multiple stages of the vacuolar transport pathway. Traffic 2, 476–486. [PubMed: 11422941]

39. Banta LM, Vida TA, Herman PK, and Emr SD (1990). Characterization of yeast Vps33p, a protein required for vacuolar protein sorting and vacuole biogenesis. Mol Cell Biol 10, 4638–4649. [PubMed: 2201898]

40. Rehling P, Darsow T, Katzmann DJ, and Emr SD (1999). Formation of AP-3 transport intermediates requires Vps41 function. Nature cell biology 1, 346–353. [PubMed: 10559961]

41. Angers CG, and Merz AJ (2009). HOPS interacts with Apl5 at the vacuole membrane and is required for consumption of AP-3 transport vesicles. Mol Biol Cell 20, 4563–4574. [PubMed: 19741093]

42. Darsow T, Katzmann DJ, Cowles CR, and Emr SD (2001). Vps41p function in the alkaline phosphatase pathway requires homo-oligomerization and interaction with AP-3 through two distinct domains. Mol Biol Cell 12, 37–51. [PubMed: 11160821]

43. Peplowska K, Markgraf DF, Ostrowicz CW, Bange G, and Ungermann C (2007). The CORVET tethering complex interacts with the yeast Rab5 homolog Vps21 and is involved in endo-lysosomal biogenesis. Dev Cell 12, 739–750. [PubMed: 17488625]

44. Bartholomew CR, and Hardy CF (2009). p21-activated kinases Cla4 and Ste20 regulate vacuole inheritance in Saccharomyces cerevisiae. Eukaryotic cell 8, 560–572. [PubMed: 19218422]

45. Arendt CS, and Hochstrasser M (1997). Identification of the yeast 20S proteasome catalytic centers and subunit interactions required for active-site formation. Proceedings of the National Academy of Sciences of the United States of America 94, 7156–7161. [PubMed: 9207060]

46. Chen P, and Hochstrasser M (1996). Autocatalytic subunit processing couples active site formation in the 20S proteasome to completion of assembly. Cell 86, 961–972. [PubMed: 8808631]

47. Stewart A, and Deacon JW (1995). Vital fluorochromes as tracers for fungal growth studies. Biotech Histochem 70, 57–65. [PubMed: 7578589]

48. Stefan CJ, and Blumer KJ (1999). A syntaxin homolog encoded by VAM3 mediates down-regulation of a yeast G protein-coupled receptor. The Journal of biological chemistry 274, 1835–1841. [PubMed: 9880567]

49. Bodnar N, and Rapoport T (2017). Toward an understanding of the Cdc48/p97 ATPase. F1000Res 6, 1318. [PubMed: 28815021]

50. Verma R, Oania R, Fang R, Smith GT, and Deshaies RJ (2011). Cdc48/p97 mediates UV-dependent turnover of RNA Pol II. Mol Cell 41, 82–92. [PubMed: 21211725]

51. Migliano SM, and Teis D (2018). ESCRT and Membrane Protein Ubiquitination. Prog Mol Subcell Biol 57, 107–135. [PubMed: 30097773]

52. Steel GJ, Laude AJ, Boojawan A, Harvey DJ, and Morgan A (1999). Biochemical analysis of the Saccharomyces cerevisiae SEC18 gene product: implications for the molecular mechanism of membrane fusion. Biochemistry 38, 7764–7772. [PubMed: 10387016]

53. Song H, Orr A, Duan M, Merz AJ, and Wickner W (2017). Sec17/Sec18 act twice, enhancing membrane fusion and then disassembling cis-SNARE complexes. Elife 6.

54. Lobingier BT, Nickerson DP, Lo SY, and Merz AJ (2014). SM proteins Sly1 and Vps33 co-assemble with Sec17 and SNARE complexes to oppose SNARE disassembly by Sec18. Elife 3, e02272. [PubMed: 24837546]

55. Neuwald AF, Aravind L, Spouge JL, and Koonin EV (1999). AAA+: A class of chaperone-like ATPases associated with the assembly, operation, and disassembly of protein complexes. Genome Res 9, 27–43. [PubMed: 9927482]

56. Vale RD (2000). AAA proteins. Lords of the ring. J Cell Biol 150, F13–19. [PubMed: 10893253]

57. Eves PT, Jin Y, Brunner M, and Weisman LS (2012). Overlap of cargo binding sites on myosin V coordinates the inheritance of diverse cargoes. J Cell Biol 198, 69–85. [PubMed: 22753895]

58. Pulgar V, Marin O, Meggio F, Allende CC, Allende JE, and Pinna LA (1999). Optimal sequences for non-phosphate-directed phosphorylation by protein kinase CK1 (casein kinase-1)--a re-evaluation. Eur J Biochem 260, 520–526. [PubMed: 10095790]

59. Marin O, Meggio F, Sarno S, Andretta M, and Pinna LA (1994). Phosphorylation of synthetic fragments of inhibitor-2 of protein phosphatase-1 by casein kinase-1 and -2. Evidence that phosphorylated residues are not strictly required for efficient targeting by casein kinase-1. Eur J Biochem 223, 647–653. [PubMed: 8055935]

60. Flotow H, Graves PR, Wang AQ, Fiol CJ, Roeske RW, and Roach PJ (1990). Phosphate groups as substrate determinants for casein kinase I action. J Biol Chem 265, 14264–14269. [PubMed: 2117608]

61. Cesaro L, and Pinna LA (2015). The generation of phosphoserine stretches in phosphoproteins: mechanism and significance. Mol Biosyst 11, 2666–2679. [PubMed: 26211804]

62. Marchal C, Haguenauer-Tsapis R, and Urban-Grimal D (2000). Casein kinase I-dependent phosphorylation within a PEST sequence and ubiquitination at nearby lysines signal endocytosis of yeast uracil permease. J Biol Chem 275, 23608–23614. [PubMed: 10811641]

63. Govindan B, Bowser R, and Novick P (1995). The role of Myo2, a yeast class V myosin, in vesicular transport. J Cell Biol 128, 1055–1068. [PubMed: 7896871]

64. Albuquerque C, Smolka M, Payne S, Bafna V, Eng J, and Zhou H (2008). A multidimensional chromatography technology for in-depth phosphoproteome analysis. Mol Cell Proteomics 7, 1389–1396. [PubMed: 18407956]

65. Lee S, Ho HC, Tumolo JM, Hsu PC, and MacGurn JA (2019). Methionine triggers Ppz-mediated dephosphorylation of Art1 to promote cargo-specific endocytosis. J Cell Biol.

66. MacGurn JA, Hsu PC, Smolka MB, and Emr SD (2011). TORC1 regulates endocytosis via Npr1-mediated phosphoinhibition of a ubiquitin ligase adaptor. Cell 147, 1104–1117. [PubMed: 22118465]

Highlights:

- Convergence of two regulatory pathways releases the vacuole from the myosin V motor

- Phosphorylation at the myosin-adaptor interface is required to release cargo

- Phosphorylation and ubiquitylation in parallel pathways release the vacuole

- Vps41 and Yck3, regulators of fusion, have independent roles in unloading vacuoles
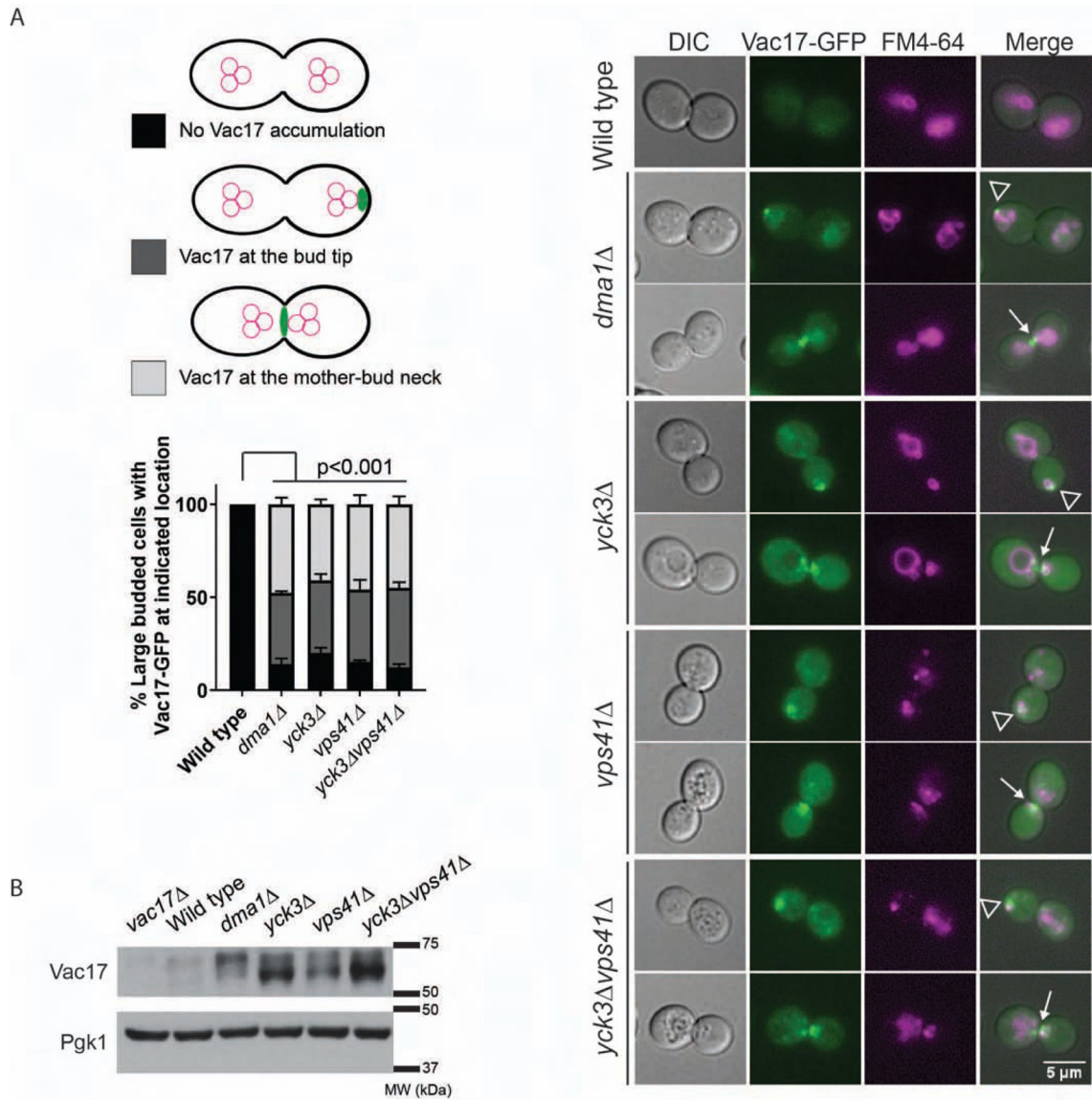
Figure 1. Yck3 and Vps41 are required for the termination of vacuole transport.

A) Similar to deletion of Dma1, deletion of Yck3 and/or Vps41 results in mislocalization of the vacuole (FM4–64) and accumulation of Vac17-GFP at the bud tip (open arrowheads) or mother-bud neck (closed arrows). Representative images of both phenotypes are shown. Wild type, *dma1*Δ, *yck3*Δ, *vps41*Δ, and *yck3*Δ*vps41*Δ mutant cells were transformed with pRS415-Vac17-GFP and labelled with FM4–64. Two-way ANOVA and Dunnett's post-hoc test. See also Figure S1.

B) Compared to wild type, endogenous levels of Vac17 are elevated in *dma1*Δ, *yck3*Δ, *vps41*Δ, and *yck3*Δ*vps41*Δ mutants.
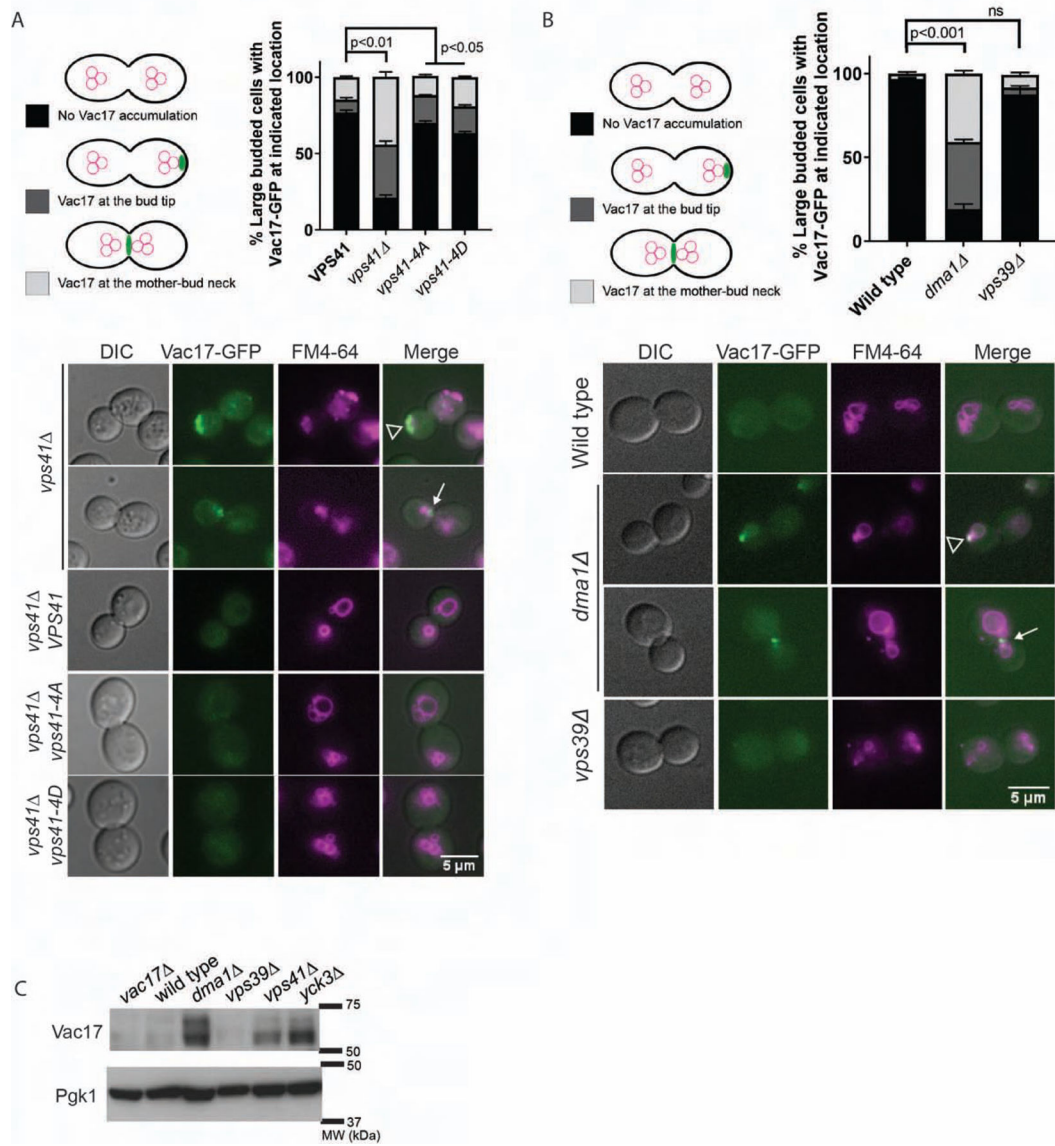
Figure 2. The HOPS complex does not have a role in the termination of vacuole transport

A) The known Yck3-dependent phosphosites on Vps41 are not essential for the release of the vacuole from Vac17 or degradation of Vac17. Vps41 mutants were scored for mislocalization of the vacuole (FM4–64) and accumulation of Vac17-GFP at the bud tip (open arrowheads) or mother-bud neck (closed arrows). *vps41* mutant cells with vector, wild type, *VPS41*, *vps41–4A*, or *vps41–4D*, was integrated into the genome. Strains were transformed with pRS415-Vac17-GFP and labelled with FM4–64. Two-way ANOVA and Dunnett's post-hoc test.

B) Unlike a deletion of Dma1, deletion of Vps39 does not result in mislocalization of the vacuole or accumulation of Vac17-GFP at the bud tip (open arrowheads) or mother-bud neck (closed arrows). Wild type, *dma1*, and *vps39* mutant cells were transformed with pRS415-Vac17-GFP and labelled with FM4–64. Two-way ANOVA and Dunnett's post-hoc test. See also Figures S2 and S3.

C) Compared with a wild-type strain, endogenous levels of Vac17 are elevated in a *dma1* mutant, but not in a *vps39* mutant.
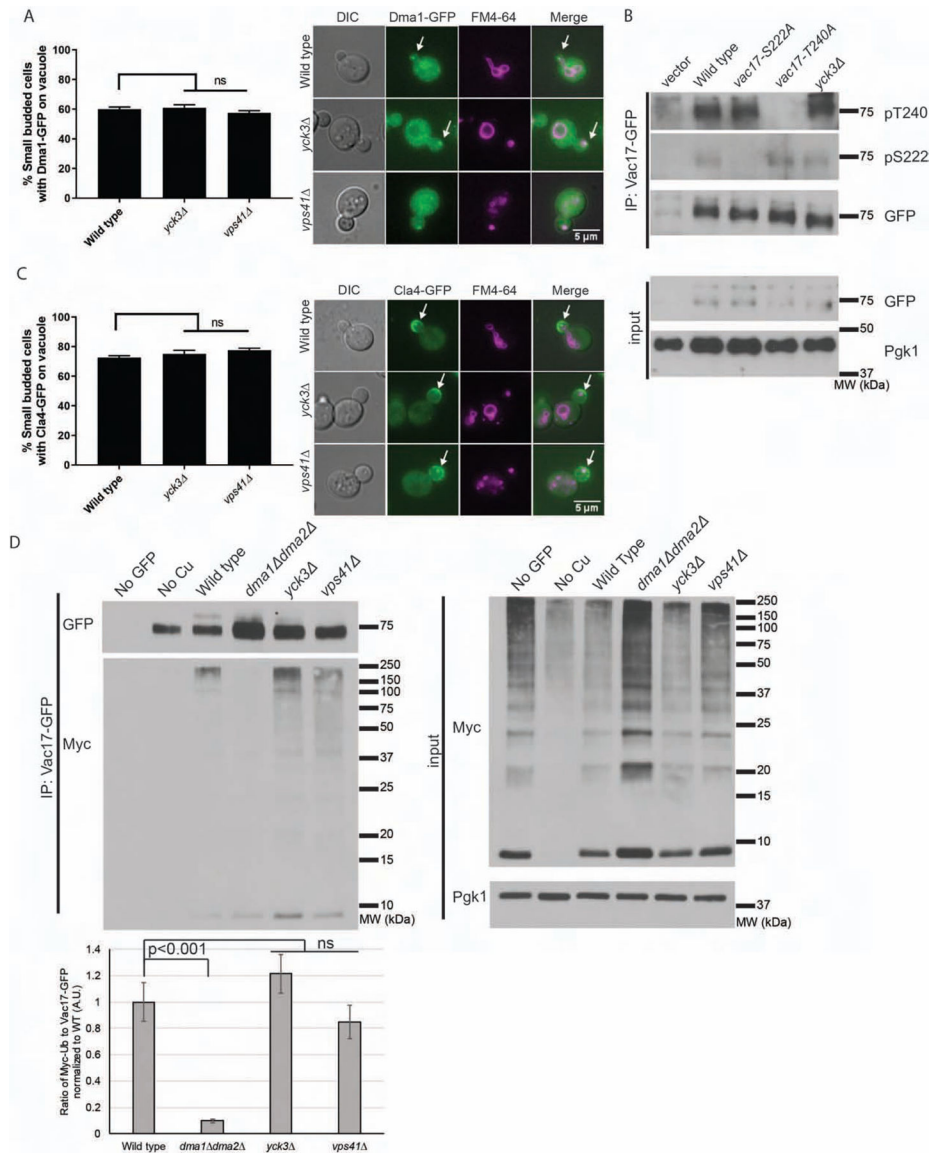
Figure 3. Yck3 and Vps41 are not required for the ubiquitylation of Vac17.

A) Dma1 is recruited to the vacuole in *yck3Δ* and *vps41Δ* mutant cells, similar to wild type (arrows). Wild type, *yck3Δ*, and *vps41Δ* mutant cells were transformed with pRS415-Vac17-GFP and labelled with FM4–64. Student's t-test.

B) Yck3 is not required for the phosphorylation of Vac17-S222 or Vac17-T240. *dma1Δ dma2Δ* (lanes 1–4) or *dma1Δ dma2Δ yck3Δ* (lane 5) mutant cells were transformed with pRS415-Vac17-GFP, *pRS415-vac17-S222A-GFP*, or *pRS415-vac17-T240A-GFP*. Vac17-GFP was immunoprecipitated with anti-GFP antibodies and analyzed via western blot.

C) Cla4 is recruited to the vacuole in *yck3Δ* and *vps41Δ* mutant cells, similar to wild type (arrows). Wild type, *yck3Δ*, and *vps41Δ* mutant cells were transformed with pRS415-Vac17-GFP and labelled with FM4–64. Student's t-test.

D) Yck3 and Vps41 are not required for the ubiquitylation of Vac17. *vac17* (lanes 1–3), *dma1 dma2 vac17* (lane 4), *yck3 vac17* (lane 5), and *vps41 vac17* (lane 6) mutant cells were co-transformed with a plasmid encoding Myc-ubiquitin under a copper-inducible promoter and pVT102u-Vac17-GFP. Vac17-GFP was immunoprecipitated using anti-GFP antibodies and analyzed via western blot. Ubiquitylation was detected via immunoblotting with anti-Myc antibody. Student's t-test.
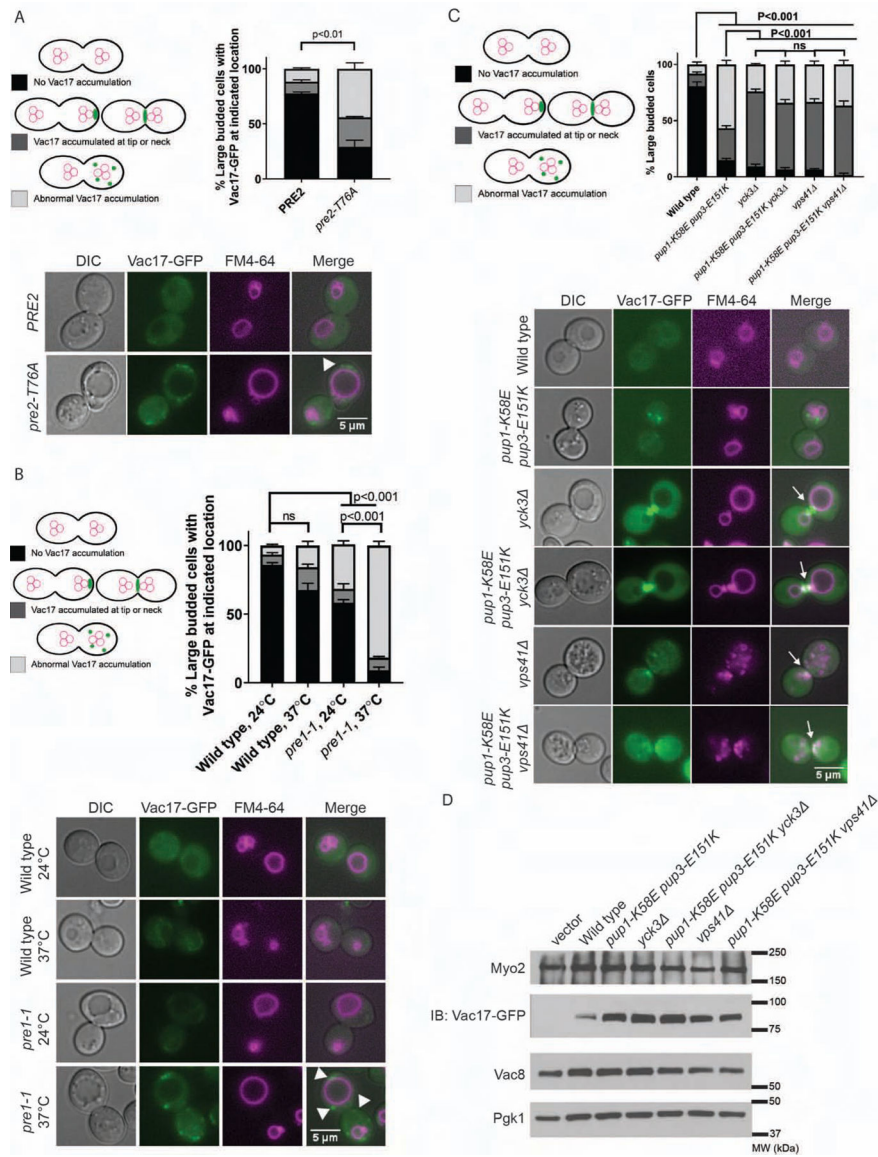
Figure 4. Yck3 and Vps41 are required to release ubiquitylated Vac17 from the Myo2-Vac17-Vac8 complex.

A) Vac17 predominately accumulates in proteasome mutants in aberrant puncta (closed arrowheads). Wild type (PRE2) and *pre2-T76A* mutant cells were transformed with pRS415-Vac17-GFP and labelled with FM4–64. Two-way ANOVA and Dunnett's post-hoc test.

B) Vac17 accumulates in aberrant puncta (closed arrowheads) in a Pre1 temperature sensitive mutant. Wild type and *pre1–1* mutant cells were transformed with pRS416-Vac17-GFP and labelled with FM4–64. Two-way ANOVA and Dunnett's post-hoc test.

C) Yck3 and Vps41 act upstream of the proteasome to release Vac17 from the vacuole. In a proteasome mutant, Vac17-GFP accumulates in aberrant puncta (closed arrowheads). However, Vac17-GFP accumulates at the bud tip or mother-bud neck (closed arrows) in *pup1-K58E pup3-E51K yck3Δ* and *pup1-K58E pup3-E51K vps41Δ* triple mutants, similar to the *yck3Δ* and *vps41Δ* mutants. Wild type, *pup1-K58E pup3-E51K*, *yck3Δ*, *pup1-K58E*

pup3-E51K yck3 , *vps41* , and *pup1-K58E pup3-E51K vps41* mutant cells were transformed with pRS416-Vac17-GFP and labelled with FM4–64. Two-way ANOVA and Tukey's post-hoc test.

D) Myo2 and Vac8 levels are not elevated or reduced in the *pup1-K58E pup3-E51K, yck3* , or *vps41* mutations. Wild type was transformed with vector or pRS416-Vac17-GFP and the other indicated strains were transformed with pRS416-Vac17-GFP. See also Figure S4 and S5.
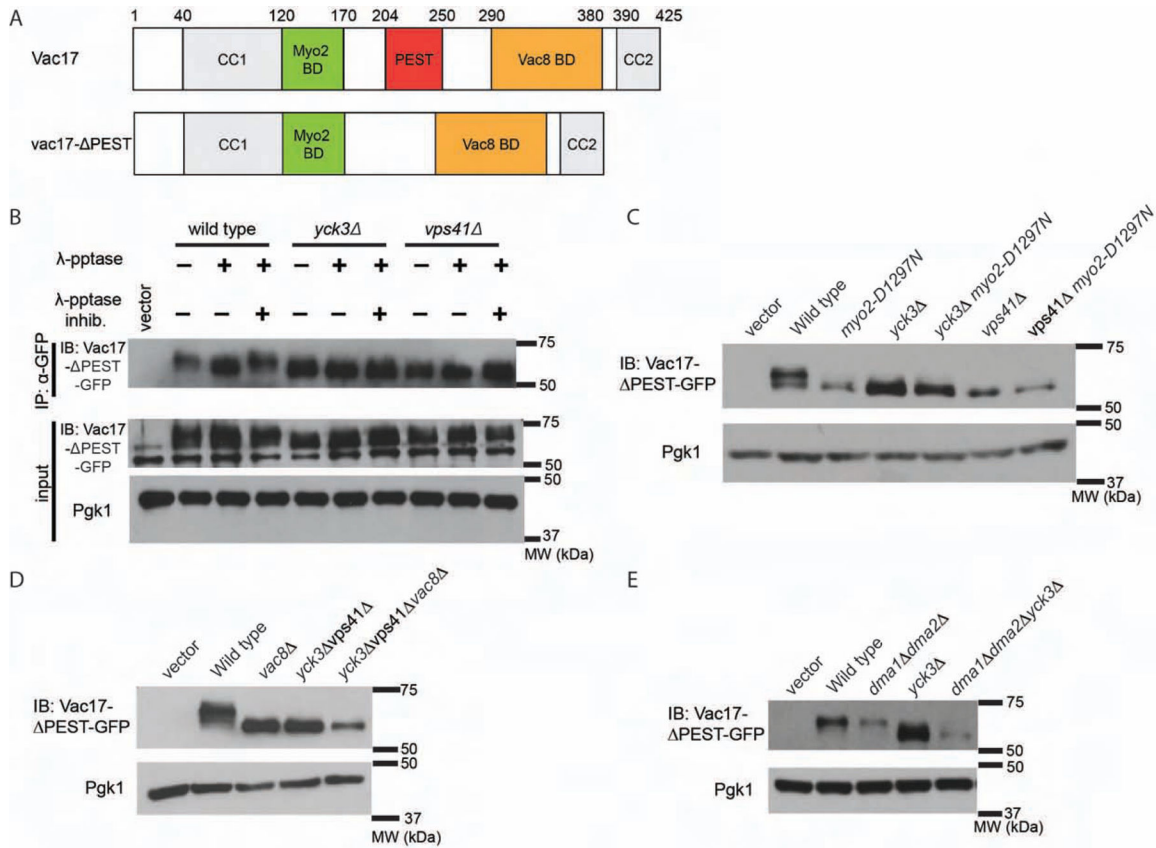
Figure 5. Yck3 and Vps41 Are Required for the Phosphorylation of Vac17

(A) Schematic of Vac17 and Vac17-ΔPEST. BD, binding domain; CC, predicted coiled coil. See also Figure S6.

(B) Yck3 and Vps41 are required for the phosphorylation of Vac17-ΔPEST-GFP. Wild-type, yck3Δ, and vps41Δ mutant cells were transformed with pRS415-Vac17-ΔPEST-GFP. λ-phosphatase treatment causes an increase in the electrophoretic mobility of Vac17-GFP in wild-type, but not yck3Δ or vps41Δ mutant, cells. Addition of phosphatase inhibitors restores the upper band in wild-type cells.

(C) Yck3- and Vps41-dependent phosphorylation of Vac17 requires binding to Myo2. vac17Δ myo2Δ, vac17Δ myo2Δ yck3Δ, and vac17Δ myo2Δ vps41Δ mutant cells were co-transformed with pRS416-Vac17-ΔPEST-GFP and either pRS413-Myo2 or pRS413-myo2-D1297N. The gel mobility of Vac17-ΔPEST-GFP was analyzed via western blot.

(D) Yck3- and Vps41-dependent phosphorylation requires Vac8. Wild-type, vac8Δ, and vac8Δ yck3Δ vps41Δ mutant cells were transformed with pRS416-Vac17-ΔPEST-GFP. The gel mobility of Vac17-ΔPEST-GFP was analyzed via western blot.

(E) Yck3-dependent phosphorylation of Vac17 does not require Dma1/Dma2. Wild-type, dma1Δ dma2Δ, yck3Δ, and dma1Δ dma2Δ yck3Δ mutant cells were transformed with pRS416-Vac17-ΔPEST-GFP and analyzed via western blot.
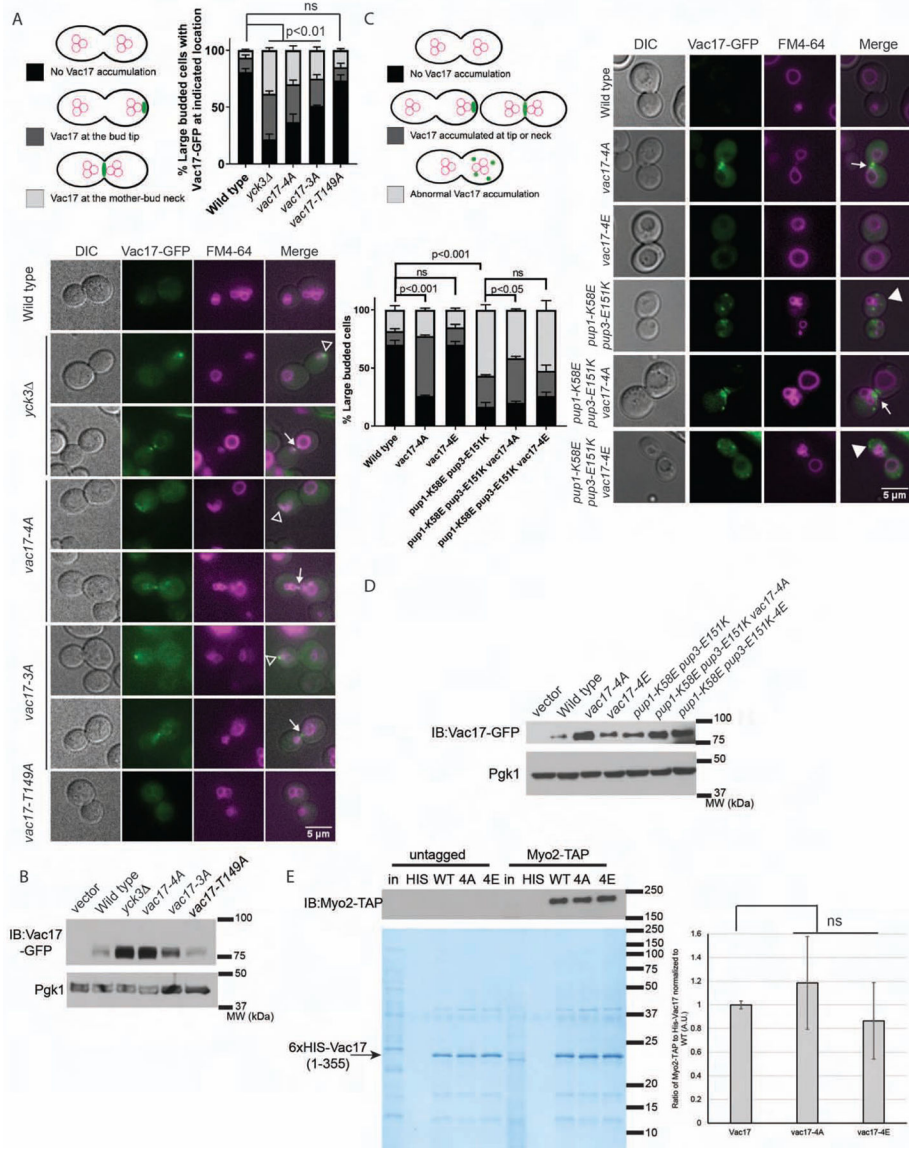
Figure 6. Yck3 and Vps41 regulate the phosphorylation of Vac17 in its Myo2 binding domain

A) Similar to deletion of Yck3, the *vac17–4A* mutant results in mislocalization of the vacuole (FM4–64) and accumulation of Vac17-GFP at the bud tip (open arrowheads) or mother-bud neck (closed arrows). *vac17Δ* or *yck3Δ vac17Δ* mutant cells were transformed with pRS416-Vac17-GFP or the Vac17 mutant indicated and labelled with FM4–64. Two-way ANOVA and Dunnett's post-hoc test.

B) The non-phosphorylatable alanine mutant, *vac17–4A*, results in elevated levels of Vac17, similar to a *yck3Δ* mutant. *vac17Δ* or *yck3Δ vac17Δ* mutant cells were transformed with pRS416-Vac17-GFP or the Vac17 mutant indicated and analyzed via western blot.

C) Vac17–4A-GFP accumulates at the bud tip (open arrowheads) or mother-bud neck (closed arrows) in wild type and the *pup1-K58E pup3-E151K* mutant. This is in contrast to the *pup1-K58E pup3-E151K* mutant, which results in Vac17 puncta (closed arrowheads). The *vac17–4E* mutant had similar phenotypes to wild type Vac17. Wild type or *pup1-K58E*

pup3-E151K mutant cells were transformed with pRS416-Vac17-GFP or the indicated Vac17 mutant and labelled with FM4–64. Two-way ANOVA and Dunnett's post-hoc test.

D) The *vac17–4A* and *pup1-K58E pup3-E151K* mutants elevate Vac17 levels above wild type. Wild type or *pup1-K58E pup3-E151K* mutant cells were transformed with pRS416-Vac17-GFP or the indicated mutant and analyzed via western blot.

E) Mutation of the four phosphorylation sites in Vac17 at the Vac17-Myo2 interface does not alter binding to Myo2. Purified recombinant HIS-Vac17(1–355), either wild type, the *-4A*, or *-4E* mutants, but not HIS alone binds Myo2-TAP from yeast lysates. 6.25% input (in). See also Figure S7.
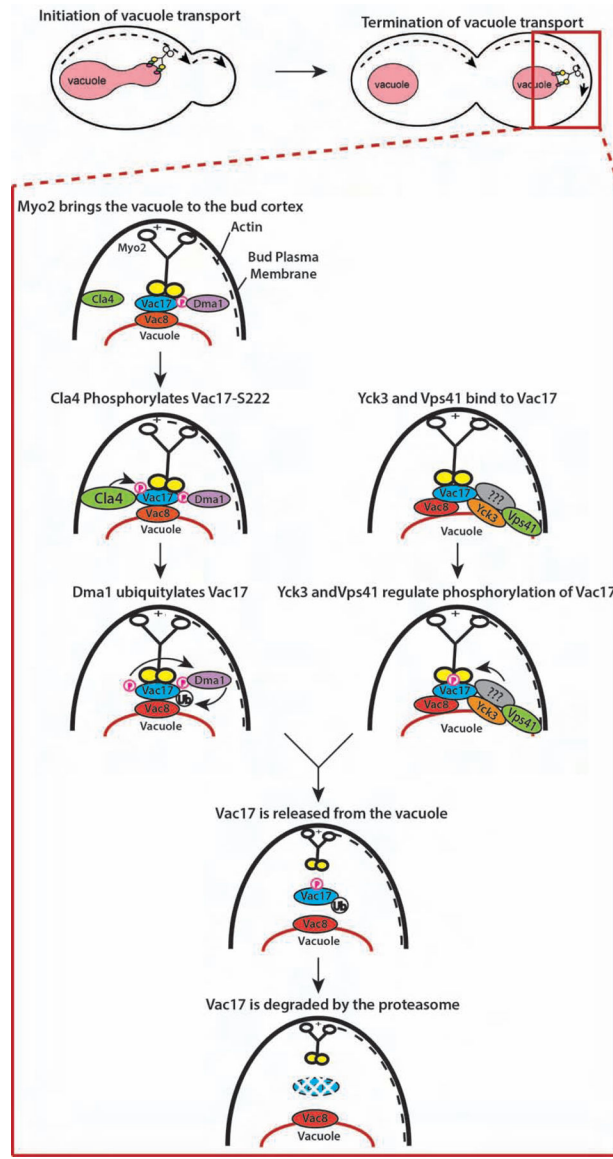
Figure 7. Model: Ubiquitylation and Yck3 and Vps41 -dependent phosphorylation are required to release Vac17 from the vacuole.

Previous studies found that Cla4 phosphorylates Vac17-S222. This phosphorylation event triggers the Dma1-dependent ubiquitylation of Vac17. In an independent and non-redundant parallel pathway, Yck3 and Vps41 are responsible for the phosphorylation of Vac17 in the Myo2 binding domain. It is likely that additional unknown regulators are required in this pathway. The integration of these two signals lead to the dissociation of the Myo2-Vac17-Vac8 complex and allow for Vac17 to be degraded by the proteasome after cargo release.

KEY RESOURCES TABLE

REAGENT or RESOURCE	SOURCE	IDENTIFIER
Antibodies		
Mouse monoclonal anti-GFP	Roche	Product #: 11814460001
Rabbit polyclonal anti-TAP	Invitrogen	Catalog #: CAB1001
Mouse monoclonal anti-Pgk1	Invitrogen	Catalog #: 459250
Rabbit polyclonal anti-GFP	Abcam	Product Code: ab6556
Rabbit monoclonal anti-Myc	Cell Signaling	Product #: 22765
Donkey Anti-Goat IgG (H+L) ML - HRP conjugated	Jackson Immuno Research	Catalog #705-035-147
Goat anti-Mouse HRP	Jackson Immuno Research	Catalog #115-035-146
Goat anti-Rabbit IgG HRP	Jackson Immuno Research	Catalog #111-035-144
Donkey anti-Sheep IgG HRP	Jackson Immuno Research	Catalog #713-035-147
Bacterial and Virus Strains		
Rosetta 2(DE3)pLysS Competent Cells	Novagen	Catalog #71403-M
OverExpress™ C43(DE3) Competent Cells	Lucigen	Catalog #60446
Chemicals, Peptides, and Recombinant Proteins		
30% Acrylamide/Bis Solution, 37.5:1	BioRad	Catalog #1610158
Pefabloc® SC	Sigma-Aldrich	SKU: 11429868001
Protease Inhibitor Cocktail for use with fungal and yeast extracts, DMSO solution	Sigma-Aldrich	SKU: P8215
cOmplete™, EDTA-free Protease Inhibitor Cocktail	Roche	SKU: 11873580001
GelCode™ Blue Stain Reagent	Thermo Scientific	Catalog #24592
PhosSTOP	Roche	SKU: 4906845001
EZview™ Red ANTI-FLAG® M2 Affinity Gel	Sigma-Aldrich	Catalh #F2426
CellTracker™ Blue CMAC Dye	Invitrogen	Catalog # C2110
SynaptoRed™ C2	Sigma-Aldrich	SKU: S6689
Lambda Protein Phosphatase	New England Biolabs	Catalog #P0753S
Trypsin Gold, Mass Spectrometry Grade	Promega	Catalog #V5280
Alpha-Factor Mating Pheromone	Zymo Research	Catalog #Y1001
Experimental Models: Organisms/Strains		
LWY3250: MAT α, ura3-52, leu2-3,-112, his3- 200, trp1- 901, lys2-801, suc2- 9	This study	N/A
LWY5798: MAT α, ura3-52, leu2-3,-112, his3- 200, trp1- 901, lys2-801, suc2- 9, vac17 ::TRP1	[17]	N/A
LYW2887: MAT α, ura3-52, leu2-3,-112, his3- 200, trp1- 901, lys2-801, suc2- 9, vac8 ::HIS3	[19]	N/A
LWY5826: MAT α, ura3-52, leu2-3,-112, his3- 200, trp1- 901, lys2-801, suc2- 9, vac17 ::TRP1, vac8 ::HIS3	This study	N/A
LWY11102: MAT α, ura3-52, leu2-3,-112, his3- 200, trp1- 901, lys2-801, suc2- 9, dma1 ::KAN	[23]	N/A

REAGENT or RESOURCE	SOURCE	IDENTIFIER
LWY11683: MAT α, ura3-52, leu2-3,-112, his3- 200, trp1- 901, lys2-801, suc2- 9, dma1 ::KAN dma2 ::KAN	[23]	N/A
LWY11687: MAT α, ura3-52, leu2-3,-112, his3- 200, trp1- 901, lys2-801, suc2- 9, dma1 ::KAN dma2 ::KAN vac17 ::TRP1	[23]	N/A
LWY11640: MAT α, ura3-52, leu2-3,-112, his3- 200, trp1- 901, lys2-801, suc2- 9, dma1 ::KAN dma2 ::KAN yck3 ::KAN	This study	N/A
LWY14777: MAT α, ura3-52, leu2-3,-112, his3- 200, trp1- 901, lys2-801, suc2- 9, vps41 ::KAN	This study	N/A
LWY14780: MAT α, ura3-52, leu2-3,-112, his3- 200, trp1- 901, lys2-801, suc2- 9, vps41 ::KAN, vac17 ::TRP1	This study	N/A
LWY10924: MAT α, ura3-52, leu2-3,-112, his3- 200, trp1- 901, lys2-801, suc2- 9, vps39 ::KAN	This study	N/A
LWY16184: MAT α, ura3-52, leu2-3,-112, his3- 200, trp1- 901, lys2-801, suc2- 9, yck3 ::KAN	This study	N/A
LWY17494: MAT α, ura3-52, leu2-3,-112, his3- 200, trp1- 901, lys2-801, suc2- 9, yck3 ::KAN vac17 ::TRP1	This study	N/A
LWY18601: MAT α, ura3-52, leu2-3,-112, his3- 200, trp1- 901, lys2-801, suc2- 9, yck3 ::KAN vps41 ::KAN	This study	N/A
LWY18556: MATa pep4 ::HIS3 prb1- 1.6R lys2-208 trp1 101 vps41 ::KANMX URA3::pRS406-NOP1pr-VPS41wt	Christian Ungermann, [34]	N/A
LWY18558: MATa pep4 ::HIS3 prb1- 1.6R lys2-208 trp1 101 vps41 ::KANMX URA3::pRS406-NOP1pr-VPS41 (S367, 368, 371, 372 A)	Christian Ungermann, [34]	N/A
LWY18560: MATa pep4 ::HIS3 prb1- 1.6R lys2-208 trp1 101 vps41 ::KANMX URA3::pRS406-NOP1pr-VPS41 (S367, 368, 371, 372 D)	Christian Ungermann, [34]	N/A
LWY10332: MAT α, ura3-52, leu2-3,-112, his3- 200, trp1- 901, lys2-801, suc2- 9, Vac17-TAP::LEU2	This study	N/A
LWY18670: MAT α, ura3-52, leu2-3,-112, his3- 200, trp1- 901, lys2-801, suc2- 9, Vac17-deltaPEST-TAP::LEU2	This study	N/A
LWY19035: MAT α, ura3-52, leu2-3,-112, his3- 200, trp1- 901, lys2-801, suc2- 9, Vac17-deltaPEST-TAP::LEU2, vps41-delta::KAN	This study	N/A
LWY19196: MAT α, ura3-52, leu2-3,-112, his3- 200, trp1- 901, lys2-801, suc2- 9, Vac17-deltaPEST-TAP::LEU2, yck3-delta::KAN	This study	N/A
LWT18737: MATα, GAL+ his3- 200 leu2-3,2-112 lys2-801 suc2- 9 trp1- 9 ura3-52	Scott D. Emr, [39]	N/A
LWT18738: MATα, vps33-4 GAL+ his3- 200 leu2-3,2-112 lys2-801 suc2- 9 trp1- 9 ura3-52	Scott D. Emr, [39]	N/A
LWY18763: MATα, vps11-delta::HIS3, pRS416-vps11-3, GAL+ his3- 200 leu2-3,2-112 lys2-801 suc2- 9 trp1- 9 ura3-52	Scott D. Emr, [38]	N/A
LWY18764: MATα, vps16-ts, GAL+ his3- 200 leu2-3,2-112 lys2-801 suc2- 9 trp1- 9 ura3-52	Scott D. Emr, [38]	N/A
LWY18765: MATα, vps18-ts, GAL+ his3- 200 leu2-3,2-112 lys2-801 suc2- 9 trp1- 9 ura3-52	Scott D. Emr, [38]	N/A
LWY7235: MATα, his3-11 leu2-3, 112 ura3-delta5 pre1-1::can	Mark Hochstrasser, [46]	N/A
LWY7236: MATα, his3-delta200 leu2-3, 112 ura3-52 lys2-801 trp1-1 doa3-delta1::HIS3[YEpDOA3LS][YCPUbDOA3deltaLS]	Mark Hochstrasser, [45]	N/A
LWY7237: MATα, his3-delta200 leu2-3, 112 ura3-52 lys2-801 trp1-1 doa3-delta1::HIS3[YEpDOA3LS][YCPUbDOA3deltaLS-T76A]	Mark Hochstrasser, [45]	N/A
LWY7238: MATα, his3-delta200 leu2-3, 112 ura3-52 lys2-801 trp1-1 pup1::leu2::HIS3 pup3-delta2::HIS3[Ycplac22PUP1][Yeplac181PUP3]	Mark Hochstrasser, [45]	N/A

REAGENT or RESOURCE	SOURCE	IDENTIFIER
LWY7239: MATα, his3-delta200 leu2-3, 112 ura3-52 lys2-801 trp1-1 pup1::leu2::HIS3 pup3-delta2::HIS3[Ycplac22pup1-K58E][Yeplac181pup3-E151K]	Mark Hochstrasser, [45]	N/A
LWY18807: MATα, his3-delta200 leu2-3, 112 ura3-52 lys2-801 trp1-1 pup1::leu2::HIS3 pup3-delta2::HIS3[Ycplac22PUP1][Yeplac181PUP3] yck3::KAN	This study	N/A
LWY18808: MATα, his3-delta200 leu2-3, 112 ura3-52 lys2-801 trp1-1 pup1::leu2::HIS3 pup3-delta2::HIS3[Ycplac22pup1-K58E][Yeplac181pup3-E151K] yck3::KAN	This study	N/A
LWY18810: MATα, his3-delta200 leu2-3, 112 ura3-52 lys2-801 trp1-1 pup1::leu2::HIS3 pup3-delta2::HIS3[Ycplac22PUP1][Yeplac181PUP3] vps41::KAN	This study	N/A
LWY18811: MATα, his3-delta200 leu2-3, 112 ura3-52 lys2-801 trp1-1 pup1::leu2::HIS3 pup3-delta2::HIS3[Ycplac22pup1-K58E][Yeplac181pup3-E151K] vps41::KAN	This study	N/A
LWY12381: MATα, can1-100, leu2-3,-112, his3-11,-15,trp1-1,ura3-1,ade2-1 cdc48-3 ts	Raymond J. Deshaies, [50]	N/A
LWY12382: MATα, can1-100, leu2-3,-112, his3-11,-15,trp1-1,ura3-1,ade2-1	Raymond J. Deshaies, [50]	N/A
LWY6470: MATα, his3 1, leu2 0, lys2 0, ura3 0	This study	N/A
LWY15465: MATα, his3 1, leu2 0, lys2 0, ura3 0, vps4- ::KAN	Horizon Discovery	Catalog ID:YSC6272-201921484
LWY14289: MATα, his3 1, leu2 0, lys2 0, ura3 0, dma1- ::KAN	Horizon Discovery	Catalog ID:YSC6272-201918767
LWY18911: MATα, his3 1, leu2 0, lys2 0, ura3 0, apl5- ::KAN	Horizon Discovery	Catalog ID:YSC6272-201918099
LWY18912: MATα, his3 1, leu2 0, lys2 0, ura3 0, aps3- ::KAN	Horizon Discovery	Catalog ID:YSC6272-201922319
LWY18913: MATα, his3 1, leu2 0, lys2 0, ura3 0, apl6- ::KAN	Horizon Discovery	Catalog ID:YSC6272-201921712
LWY18665: MATα, his3 1, leu2 0, lys2 0, ura3 0, vps3- ::KAN	Horizon Discovery	Catalog ID:YSC6272-201920493
LWY18666: MATα, his3 1, leu2 0, lys2 0, ura3 0, vps8- ::KAN	Horizon Discovery	Catalog ID:YSC6272-201917680
LWY19052: MATα, his3 1, leu2 0, lys2 0, ura3 0, apm3- ::KAN	Horizon Discovery	Catalog ID:YSC6272-201922619
LWY19425: MATα, his3 1, leu2 0, lys2 0, ura3 0, sec18-DAmP::KAN	Horizon Discovery	Catalog ID:YSC5094-213595288
LWY19072: MAT α, leu2-3,112 ura3-52 his3- 200 trp1- 901 suc2- 9 lys2-801, arg4::KAN, pVT102u-Vac17-deltaPEST-FLAG, pRS413-Myo2-D1297N	This study	N/A
LWY19073: MAT α, leu2-3,112 ura3-52 his3- 200 trp1- 901 suc2- 9 lys2-801, arg4 ::KanMX, vps41 ::KanMX, pVT102u-Vac17-deltaPEST-FLAG, pRS413-Myo2-D1297N, vps41-KO	This study	N/A
LWY19074: MAT α, leu2-3,112 ura3-52 his3- 200 trp1- 901 suc2- 9 lys2-801, arg4 ::KAN, yck3 ::KanMX, pVT102u-Vac17-deltaPEST-FLAG, pRS413-Myo2-D1297N, yck3-KO	This study	N/A
LWY8382: MAT α, ura3-52, leu2-3,-112, his3- 200, trp1- 901, lys2-801, suc2- 9, Myo2-TAP::KAN	This study	N/A
Recombinant DNA		
pRS415-Vac17-GFP	[17]	N/A
pRS416-Vac17-GFP	[17]	N/A
pRS416-Vac17-4A-GFP	This study	N/A
pRS416-Vac17-3A-GFP	This study	N/A
pRS416-Vac17-T149A-GFP	This study	N/A
pRS416-Vac17-4E- GFP	This study	N/A
pRS415-Vac17- PEST	[17]	N/A

REAGENT or RESOURCE	SOURCE	IDENTIFIER
pRS416-Vac17- PEST	[17]	N/A
pRS416-Vac17- PEST-GFP	[17]	N/A
pRS416-Dma1-GFP	[23]	N/A
pRS413-Cla4-GFP	[23]	N/A
pRS413-Myo2-Venus	[23]	N/A
pRS416-Myo2-Venus	This study	N/A
pRS413-Myo2-D1297N	[57]	N/A
pRS413-mCherry-Myo2	This study	N/A
pRS406-VPS41pr-Vps41-WT	Christian Ungermann, [34]	N/A
pRS406-VPS41pr-Vps41-4A	Christian Ungermann, [34]	N/A
pRS406-VPS41pr-Vps41-4D	Christian Ungermann, [34]	N/A
CUP1-Myc-Ubiquitin	[23]	N/A
pvt102u-Vac17-GFP	[23]	N/A
pvt102u-Vac17	[23]	N/A
pVT102u-Vac17- PEST-6xHis-TEV-3xFLAG	This study	N/A
pGEX-Yck3 (2-516)	This study	N/A
pSAP0162 (pQLinkHM-Vps41 (124-992)	This study	N/A
pET28a-Vac17(1-355)	This study	N/A
pET28a-Vac17(1-355)-4A	This study	N/A
pET28a-Vac17(1-355)-4E	This study	N/A
Software and Algorithms		
ImageJ	National Institutes of Health	https://imagej.net/Fiji/Downloads
MaxQuant (ver. 1.6.5.0)	MaxQuant	maxquant.org
Skyline (ver. 19.1.0.193)	MacCoss Lab	skyline.ms
PRISM (ver 8.0.2(263))	GraphPad	graphpad.com/scientific-software/prism